THERMAL OXIDATION BEHAVIOUR OF SOFTWOOD KRAFT LIGNIN

Lappeenranta–Lahti University of Technology LUT

Master's Programme in Chemical Engineering, Master's thesis

Master's programme in Biorefineries

2024

Jarno Vepsäläinen

Examiners: Docent Ikenna Anugwom, D.Sc. (Tech.)

Mario Wachtler, Dr. techn. Director of Product Development Lignode

ABSTRACT

Lappeenranta–Lahti University of Technology LUT

LUT School of Engineering Sciences

Chemical Engineering

Jarno Vepsäläinen

THERMAL OXIDATION BEHAVIOUR OF SOFTWOOD KRAFT LIGNIN

Master's thesis

2024

50 pages, 21 figures, 4 tables and 7 appendices

Examiner(s): Docent Ikenna Anugwom and Mario Wachtler, Dr. techn. Director of Product Development Lignode

Keywords: lignin, softwood, kraft, oxidation, thermal treatment, heat treatment, cross-linking, glass-transition temperature, T_g, DSC

Lignin-derived carbon materials has been a keen topic of research in recent years. Lignin is thermally degraded in pyrolysis, a process called carbonization, into a variety of liquid and gaseous compounds and solid residue. The solid residue, called carbon or biochar, is used for carbon products. Lignin, however, has a complex structure and chemical composition making processing challenging, and lignin has a tendency to melt in high temperatures of pyrolysis.

This thesis examines the physico-chemical changes in softwood kraft lignin using thermal oxidation (TO) process. During TO treatment, thermoplastic lignin is treated at relatively low temperatures in the presence of air, which modifies the physical properties of the lignin to thermoset material, making it infusible and easier to process in pyrolysis temperatures.

A full-factorial design of experiment (DOE) was performed for three factors (temperature, time and heating rate) to see main effects on the material properties and to find optimal process conditions in TO treatment for softwood kraft lignin. Analytical methods include organic elemental analysis, thermogravimetric analysis and modulated differential scanning calorimetry. Regression models were made for the results, main effects for each response identified and response optimization including significant analyses was created to identify optimal process conditions.

ACKNOWLEDGEMENTS

I would like to thank my supervisor Mario Wachtler for his guidance on this journey, Abhishek Shetty for new insights along the way and Lidia Marquino Fernandez for great tutoring on data analysis.

Special thanks to material analysis team, especially Busra Keles and Runa Ekberg, who helped me with the material analysis.

Jarno Vepsäläinen

13.6.2024

SYMBOLS AND ABBREVIATIONS

Greek characters

α	confidence level	

Abbreviations

CF	carbon fiber	
C%	carbon content	[m-%]
HR	heating rate	ºC/min
HT	holding time at max. temperature	h
MM	molar mass	
MT	maximum temperature	°C
OEA	organic elemental analysis	
O%	oxygen content	[m-%]
PAN	polyacrylonitrile	
T_g	glass-transition temperature	°C
TO	thermal oxidation	

Table of contents

Abstract

Acknowledgements

Symbols and abbreviations

1 Introduction 7
2 Lignin 9
2.1 Structure and composition of lignin 9
2.2 Lignin extraction 11
2.3 Lignin applications 13
3 Lignin degradation and structure modification 15
3.1 Lignin depolymerization 15
3.1.1 Thermal degradation 17
3.2 Thermal Oxidation 18
3.2.1 Crosslinking 18
3.2.2 Glass-transition temperature T_g 19
4 Design of experiments 21
4.1 Research layout 21
4.2 Equipment and materials 24
4.3 Analytical methods & sample preparation 25
4.3.1 OEA 25
4.3.2 XRF 26
4.3.3 DSC 26
4.3.4 TGA 28
4.3.5 Yield after TO treatment 29
5 Results and discussion 29
5.1 MDSC 31
5.1.1 Glass-transition temperature 31
5.1.2 Reaction energy heat flow 33
5.2 Elemental analysis 35

5.2.1 Carbon content C% 35
5.2.2 Oxygen content O% 36
5.2.3 Other elements 37
5.3 TGA 38
5.4 TO treatment yield 39
5.5 Optimal process parameters 40
Conclusions 44
References 48

Appendices

Appendix 1. Comparison of MDSC data

Appendix 2. Factorial regression of glass-transition temperature T_g

Appendix 3. Factorial regression of carbonization yield

Appendix 4. Factorial regression of carbon content

Appendix 5. Factorial regression of oxygen content

Appendix 6. Factorial regression of reaction energy

Appendix 7. Factorial regression of TO treatment yield

1 Introduction

Since the 19th century, fossil fuels have been utilized as an energy source and as a raw material for chemicals. The demand for limited fossil fuels has grown to unsustainable levels over the years, and alternative resources to replace fossil fuels have started to gain interest.

Woody biomass is a promising and low-cost renewable resource to reduce our dependence on fossil fuels. For centuries, a wide range of products has been utilizing wood in construction and energy, and cellulose in pulp and paper industry. But lignin, the second most abundant biopolymer after cellulose, has mostly been utilized in power and heat production in pulp mills.

In pulp production, lignin is separated from cellulose in the kraft cooking process into a stream of organic matter and cooking chemicals called black liquor and burned for energy. Lignin can also be separated from black liquor to be used as energy elsewhere or as a raw material for potentially more value-added applications.

In recent decade many studies on lignin valorization have been conducted, since lignin is seen as a potential candidate for e.g. biochemicals, biopolymers and carbon products. Low-cost, abundancy and renewability make lignin a desirable raw material source, but it also has a complex structure and heterogeneous chemical composition, which makes characterizing and processing lignin challenging (Bajwa et al., 2019).

Thermal treatment at high temperatures enhances the morphological, mechanical, and electromagnetic properties of lignin, and transform it into new materials, such as value-added carbon products e.g., carbon fibers (CF) and hard carbon anode materials for batteries.

This thesis examines the physico-chemical changes in softwood kraft lignin using thermal oxidation (TO) process. During TO treatment, thermoplastic lignin is treated at relatively low temperatures in the presence of oxygen or air, which modifies the physical properties of the lignin by introducing oxygen containing functional groups and cross-linking bonds, turning the treated lignin into thermoset material. Lignin has a tendency to melt during thermal treatment in high temperatures making processability challenging, thermosetting lignin produces an infusible and insoluble polymer network improving processability (Bhattacharyya, et al., 2020; Beste, A., 2014).

Other studies on TO treatment mostly focus on polyacrylonitrile (PAN) fibers as precursors for CF production, but some were found for lignin-based CF. Studies about TO for other applications than CF are scarce. One of the few Du et al. (2020) studied pre-oxidation of sodium lignosulfonate lignin for hard carbon battery materials.

Nevertheless, the TO treatment works according to the same principle for other polymers as for lignin, so these studies can give us indication about reactions happening in the TO treatment of this study.

In this study, a full-factorial design of experiment (DOE) is performed to find optimal process conditions in TO treatment for softwood kraft lignin. The three key parameters identified are temperature, holding time at maximum temperature and heating rate. The impact of each parameter on the degree of TO is investigated, which is evaluated with changes in glass transition temperature T_g measured with modulated differential scanning calorimetry (MDSC). T_g is expected to rise significantly when cross-linking is introduced. Other relevant measurements to investigate the TO treatment are thermogravimetric analysis (TGA) and analysis of organic elements (OEA), especially carbon (C%) and oxygen content (O%). Statistical analysis of the results and graphs are made with Minitab software.

The thesis aims to look for answers in the following questions:

- How does the thermal oxidation (TO) treatment key parameters affect the material properties?
- Which factors does the T_g value measured with MDSC correlate with?
- Can we determine optimal key parameter settings to produce well performing oxidized lignin with minimal time for the TO treatment step?

The purpose of finding optimal conditions is of great importance for the thermal treatment of lignin in high temperatures to decrease production costs and to improve lignin-based carbon properties. Also, learnings about impact of temperature, holding time and heating rate may help to better understand kraft lignin as a raw material for carbon products.

The scope of the thesis is limited to a study of the TO treatment and the properties of the resulting materials. Further processing of the TO-treated lignin as well as the final carbon products are not part of the thesis. In the following chapters I dig into lignin, its thermal

degradation and crosslinking as a phenomenon. Then set up a DOE study, describe analysis methods and sample preparation, show results, and conclude the study.

2 Lignin

This chapter describes lignin structure and composition and briefly reviews lignin extraction methods as a raw material for different applications and value-added products. Lignin applications will describe lignin utilization today and emerging applications. We will also shortly discuss challenges present in lignin extraction and utilization in different applications. By natural lignin, we refer to the composition of lignin in the cell wall, and by technical lignin, the composition of extracted lignin.

2.1 Structure and composition of lignin

Natural lignin is biopolymer that contributes greatly to the formation of the cell walls of plants. Chemically, lignin is a phenolic polymer with a complex, heterogenous and amorphous macromolecular structure and it is formed by radical coupling polymerization of three lignin monomers (monolignols); p-coumaryl, coniferyl and sinapyl alcohols, which link together in an unorderly manner. The structure and content ratio of each monolignol in lignin is dependent on the wood source. Figure 1 presents the three monolignols and their monomeric units. In softwood lignin, the predominant building block is the coniferyl alcohol unit (Xu & Ferdosian, 2017).

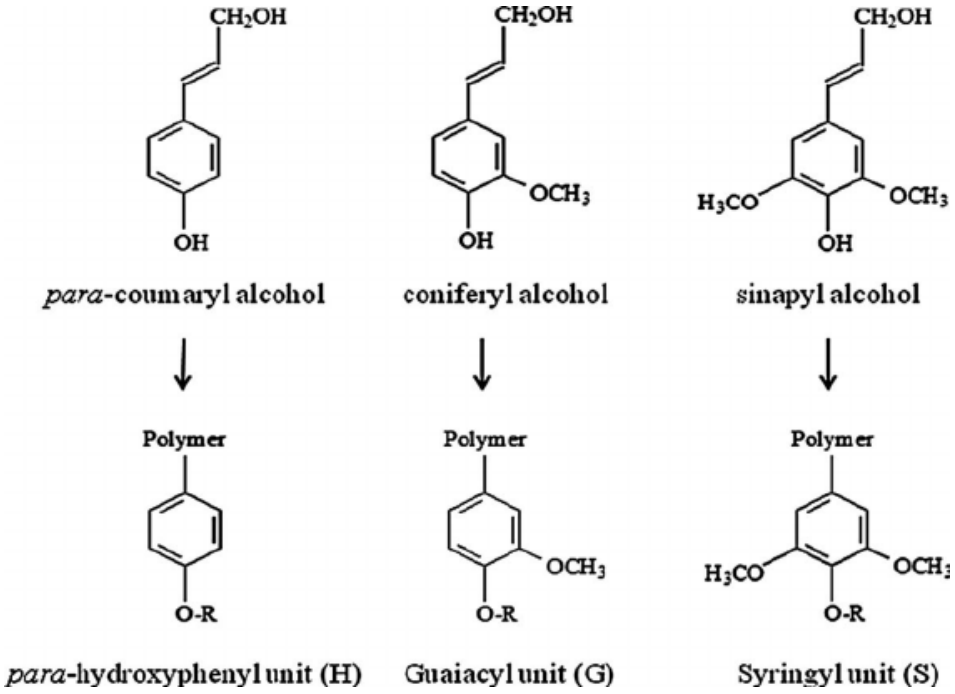

Figure 1. Monolignols and monomeric units (Moon†, Dahyun & Shin, Soo-jeong & Choi, Joon & Park, Jong-Sug & Kim, Wook & Kwon, Mi. (2011). Chemical modification of secondary xylem under tensile stress in the stem of Liriodendron tulipifera. Forest Science and Technology. 7. 53-59. 10.1080/2158010)

Monolignols are interconnected to one another by linkages, and up to two-thirds of all of the linkages present in the lignin structure consist of C-O-C ether bonds (β-O-4, α-O-4, 4-O-5), and the rest are mostly aliphatic C-C bonds (β-5, 5-5, β-1, β- β), as seen in Figure 2. Most common β-O-4 bonds, which can make up approx. 46–60% of all linkages depending on the source of wood. The linkages form a 3D network structure of phenolic units, and the natural lignin structure is also dependent on the wood source, location, season etc. This 3D network structure plays an important role in the transformation of lignin to chemicals and materials, so different sources and process methods of lignin may work better for different products. Different analytical methods such as FTIR, NMR and GPC have been commonly used in investigation of the lignin structure (Xu & Ferdosian. 2017).

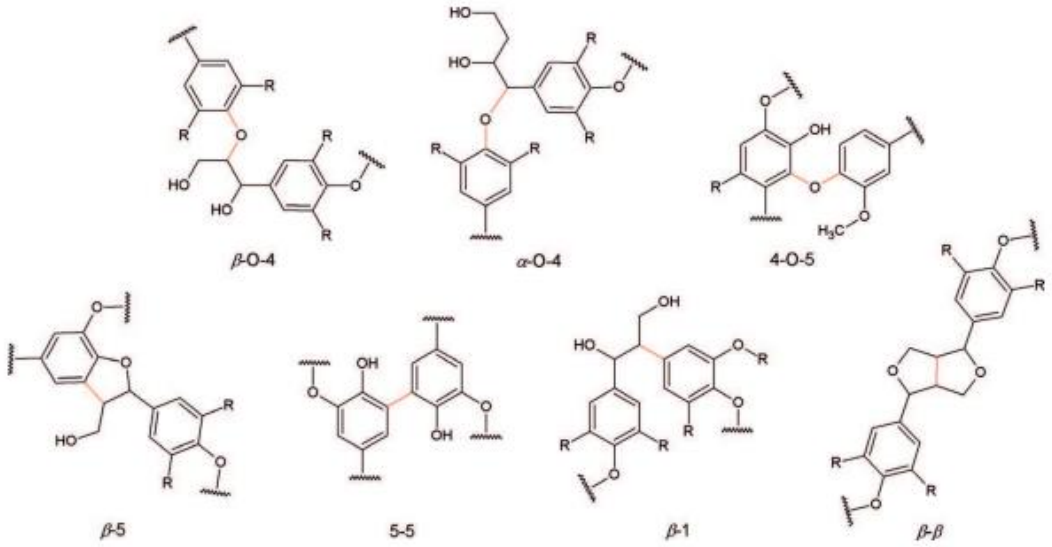

Figure 2. Characteristic bonds occurring in the structure of lignin (Poletto, 2018)

Lignin macromolecules also contain various functional groups, such as methoxy, hydroxyl, carbonyl and carboxyl groups, which affect their reactivity. Most hydroxyl groups form bonds with adjacent structural units, so only some are free to react. (Poletto, 2018)

2.2 Lignin extraction

Lignin can be extracted from lignocellulosic biomass by chemical, biochemical, and physical processes. As mentioned, the chemical structure and properties of the lignin are depended on the lignin source (plant species) but also depended on the extraction method. By technical lignin we refer to the extracted lignin, where the lignin structure and properties have been modified (i.e. undergone degradation) compared to natural lignin due to various treatment steps e.g., delignification (Braun et al., 2005).

Extraction types can be classified in several ways, first into sulfur and sulfur-free processes or processes dissolving lignin into a solution, and processes hydrolyzing cellulose and hemicellulose in acid or organic solvents leading to separation of lignin as an insoluble residue (Figure 3).

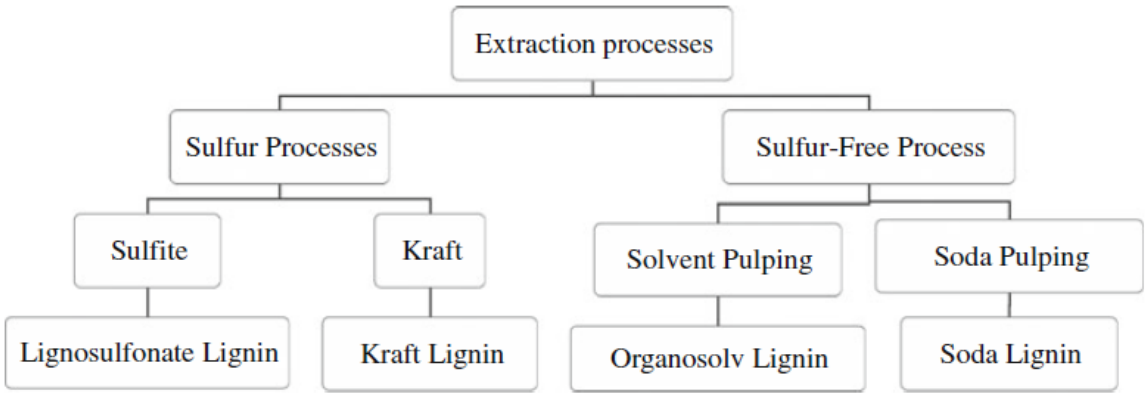

Figure 3. Most common lignin extraction processes (Xu & Ferdosian, 2017)

Traditionally technical lignin is obtained as a by-product of industrially dominant kraft pulp mills, where the process is optimized for the qualitative and quantitative yield of cellulose pulp (Ekielski & Mishra, 2021).

Xu & Ferdosian (2017) describe the extraction process of alkali lignin, where lignin is exctracted from the biomass in the NaOH solution at high temperature and pressure. In this cooking process the intermolecular linkages to polysaccharides are broken and lignin fragments are dissolved in the solvent, called black liquor. The lignin is then separated from the black liquor with Na_2CO_3 (soda lignin) or Na_2SO_4 (kraft lignin).

Other common lignin dissolving methods include the Sulfite & Organosolv pulping processes. Methods isolating lignin the insoluble residue include enzymatic hydrolysis method, where polysaccharides linkages are hydrolyzed into fermentable sugar and the resulting residue is called hydrolytic lignin and the Klason method, where polysaccharide linkages are hydrolyzed with 72% sulfuric acid. Klason method, however, is mainly used for determination of lignin content in wood (Xu & Ferdosian, 2017).

In Figure 4 Suota et al. (2021) have quantified lignin monomers and inter-units of softwood and hardwood lignin extracted with the Lignoforce™ process.

Lignin structural quantification per 100 C9 units	LFHL	LFSL
Lignin monomers		
Syringyl (S)	66.3	nd[2]
Guaiacyl (G)	33.7	96.2
p-Hydroxyphenyl (H)	nd	3.8
S/G ratio	1.97	nd
H/G ratio	nd	0.03
Lignin inter-units		
Aryl ether (β-O-4′)	6.2	5.8
Phenylcoumaran (β-5′)	0.2	1.7
Resinol (β-β')	3.6	2.1
Epiresinol (β-β')	1.6	0.3
Seicosolariciresinol (β-β')	nd	1.6
Stilbene (β-1′)	1.0	0.5
Stilbene (β-5′)	2.1	8.1
Lignin end-groups		
Cinnamyl alcohol	nd	1.4
Cinnamaldehyde	0.8	2.0
p-Hydroxybenzoate	0.6	nd
Ferulate	1.2	2.1
Others		
Methoxyl[1]	185	117
Xylose	0.4	0.6

Figure 4. Quantification of major substructures in LFHL (Hardwood) and LFSL (Softwood), with their relative abundance expressed in relation to 100 lignin monomers (Suota et al., 2021)

2.3 Lignin applications

As mentioned, the complex structure of lignin is still not completely understood and the classification of lignin characteristics has not been sufficient due to varying data, which is why lignin has had a limited utilization possibility, e.g. in heat and power generation. Bajwa et al. (2019) highlights that less than 2% of the lignin produced by the paper industry is sold for production of value-added chemicals, such as adhesives, surfactants and dispersants. The complex structure of lignin, high chemical stability, and the fact that methods for its modification and depolymerization are still quite expensive and challenging to carry out on

an industrial scale, significantly restricting its applications. Cheap, efficient, and simple technologies to degrade lignin into useful bioproducts are in high demand.

Every delignification method modifies the structure of lignin in its specific way. The properties of technical lignin directly affects the suitable applications. Kraft lignin for example, contains sulphur residuals from lignin separation, that are considered impurities limiting the valorization of technical lignin. Organosolv lignin on the other hand, are high purity lignin with lower-molecular-weight fragments, which is expected to be advantageous in blending lignin with thermoplastic polymers and higher solubility with organic solvents, such as filler in paints or inks (Suota et al., 2021).

Important properties for many applications are e.g., the extent of C-C bond cleavage, condensation degree, molecular weight, and variations (quantitative and qualitative) in functional groups. The presence of various functional groups on lignin, e.g., aromatic compounds (C-H bonds) and hydroxyl groups (-OH) make it as a potential candidate for the synthesis of bio-aromatic chemicals, such as vanillin and phenols, and bio-based polymeric materials (polymers and resins) (Xu & Ferdosian, 2017).

Suota et al. (2021) also found that hardwood lignin extracted in the Lignoforce™ process has a lower molecular mass compared to softwood lignin. The potential applications between hardwood and softwood can be separated based on these properties since lower molar mass (MM) is expected to be advantageous in blending lignin with thermoplastic polymers and higher solubility with organic solvents. The high total -OH groups in combination with high solubility with organic solvents also suggests suitability of hardwood lignin for replacement of isocyanate adhesives in wood products and petroleum-based polyols in the preparation of polyurethane foams. Softwood lignin was seen as suitable replacement of phenol in phenol formaldehyde resins, and its higher MM and improved thermal stability are seen to be useful in making carbon products, as well as producing chemicals like vanillin.

Lignin has also become commonly used in the preparation of multifunctional hybrid systems in the last decade. Poletto (2018) reports several examples concerning silica–lignin materials, which may be used as polymer fillers, effective and relatively cheap sorbents of environmentally hazardous metal ions, systems with antibacterial properties, components in abrasive products, etc. There are also reports of hybrid systems in which lignin is combined with titanium dioxide, magnetite, and the oxide systems, as well as chitin. All these systems

can be used as effective sorbents of environmentally hazardous metal ions, and the chitin-lignin system can also be used as an enzyme carrier.

Several studies mentioned in this thesis also discuss the lignin utilization in CF precursors. Beste, A., (2014) points out that polymers reinforced with CF has found extensive use in high-end applications such as in sporting goods or aerospace. CF production is limited by high production cost and the fact that PAN is derived from fossil fuels. Low-cost and renewable lignin is a promising alternative to overcome these disadvantages, provided that lignin processability and mechanical characteristics can be improved.

Other recent studies of lignin-based carbon applications are reviewed by Chatterjee & Saito (2015), where some highlights are activated carbon for applications, such as gas separation and filtration and CF mats for well performancing anode materials for Li-ion batteries. Lin et al. (2020) also explored lignin as a precursor for hard carbon anodes in Na-ion batteries.

3 Lignin degradation and structure modification

In this chapter, lignin depolymerization and thermal degradation by pyrolysis is introduced. Pyrolysis is the main process pathway for carbon-based applications. Chapter 3.2 discusses the TO treatment as a method to thermally modify the lignin structure and to change thermoplastic lignin into an infusible thermoset material.

3.1 Lignin depolymerization

To obtain the precious monomers used in lignin-derived products, lignin needs to be exposed to a process called depolymerization, which aims to decompose the biopolymer into monomers by breaking the intermolecular bonds. There are various depolymerization methods, including chemical, biological, thermal methods or combinations of these, using catalysts and high temperatures. The depolymerization method largely affects what compounds and in what yields are obtained. The most important low-molecular components are shown in Figure 5 (Poletto, 2018).

Poletto (2018) summarizes studies, that have determined the effective methods of depolymerization leading to large number of phenolic monomers. The most important of these methods includes pyrolysis process, the use of metallic, acidic or alkaline catalysts, ionic liquids and supercritical fluids in lignin depolymerization.

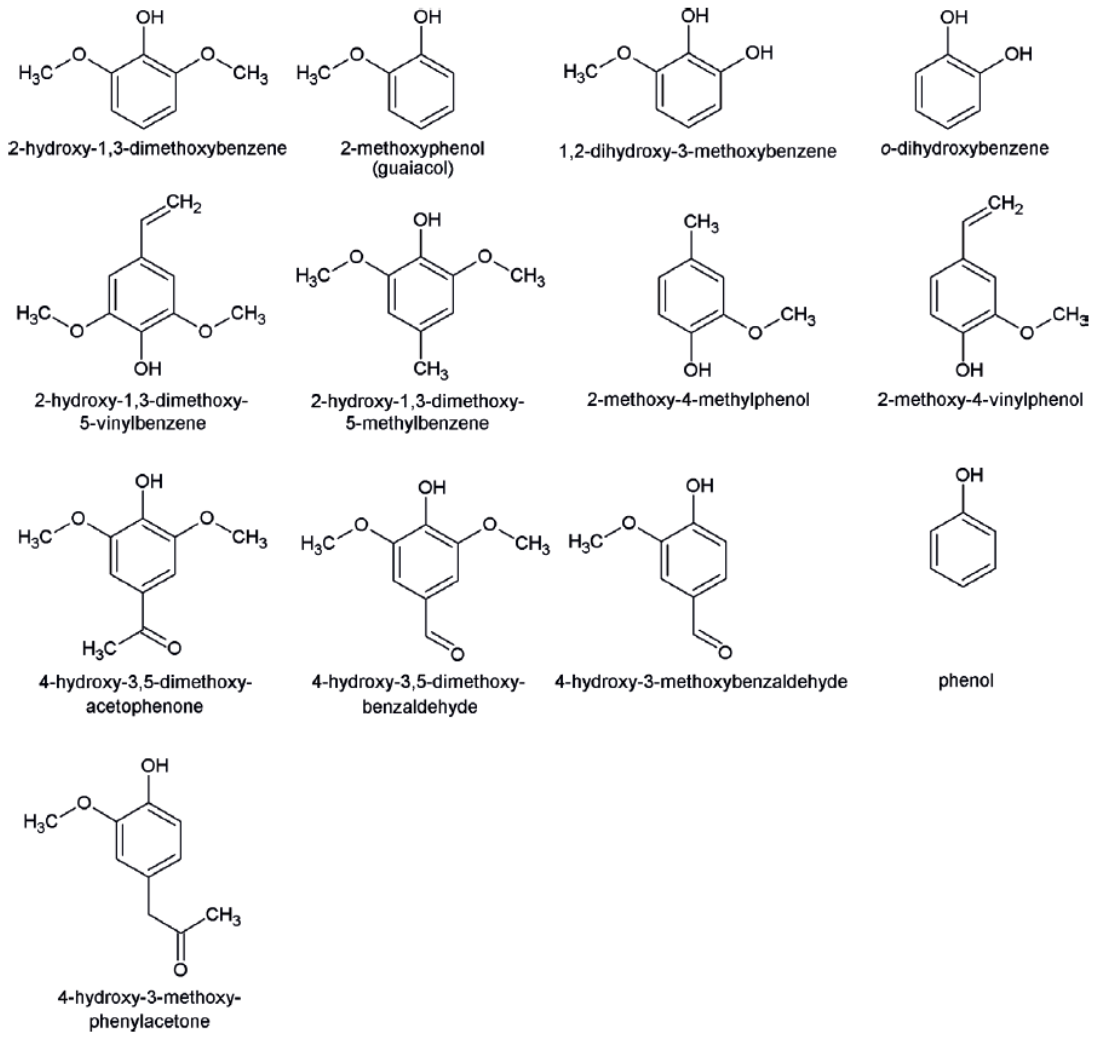

Figure 5. The most important low-molecular-weight compounds obtained from the depolymerization of lignin (Poletto, 2018)

Depolymerization of lignin with mentioned methods above, the following fractions are obtained in different portion and depending on used depolymerization method. The solid residue (carbon, residual lignin), liquid fraction (oil, alcohols) and oligomers. The residual lignin consists of remaining particles which have not decomposed or have potentially repolymerized. Oils are a mixture of phenolic monomers, such as 2-hydroxy-1,3-

dimethoxybenzene and guaiacol. In some cases, liquids may contain alcohols, as well as hydrophilic aromatic compounds which cannot be isolated. Oligomers contain a lot of chemical compounds needed by different industries so it is wanted for many applications. The quantity and composition of each fraction depends on the process conditions.

3.1.1 Thermal degradation

Pyrolysis of lignin is one of the methods for lignin depolymerization. In pyrolysis, lignin is introduced to high temperatures in inert atmosphere (without oxygen). The high temperature causes cracking of the ether- and C–C bonds, and the inert atmosphere prevents oxidation of the lignin. The process leads solid residue for carbon products, liquid products containing monomeric phenolic compounds and gaseous compounds consisting mainly of oxides of carbon (CO, CO_2) and hydrocarbons. The proportions of compounds depend on the process conditions (Table 1). After reaching 500°C, aromatic ring bonds are broken and hydrogen is formed. This process step is also called gasification, and gases can account for more than 80% of the products in certain conditions (Poletto, 2018).

Type of pyrolysis	Residence time	Temperature (°C)	Yield (%)		
			Liquid	Char	Gas
Slow	Hours/Days	500	10	30	40
Fast	~ 1–2 s	500	60	10	15

Table 1. Product yield of two types of pyrolysis (Poletto, 2018)

Xu & Ferdosian (2017) also reported that hardwood lignin pyrolysis produces more liquid products compared to softwood lignin, which can be explained by more β-O-4 bonds on the hardwood lignin that are weaker than the C–C bonds in softwood lignin. The dominating products of the softwood lignin pyrolysis are guaiacyl compounds due to the lack of syringyl units in the structure of the softwood and the maximum of phenol yield was obtained at 600 °C.

The resulting liquid fraction of lignin is mostly oil, but has a disadvantage of containing many oxygen compounds, which means that it cannot be used as a fuel. However, Poletto (2018) shares that research is being done with the aim of improving the pyrolysis process by reducing the number of organic oxide compounds by adding polyolefin to the pyrolysis

process and increasing the content of phenolic compounds in the oil by adding polystyrene to the pyrolysis process.

3.2 Thermal Oxidation

Pyrolysis at high temperatures gradually transforms lignin into carbon, and thereby enhances the morphological, mechanical, and electromagnetic properties of material, when aiming for value-added carbon products such as carbon fibers (CF) and hard carbon anode materials for batteries. However, lignin has a tendency to melt during heat treatment, making it relatively hard to process. In order to prevent melting, the lignin properties need to be modified. Thermal oxidation (TO) or as Yuan et al. (2017) and Braun et al. (2005) refer to as oxidative stabilization or oxidative thermostabilization, has been studied as a method to change the lignin structure, with the resulting lignin becoming more resistant to thermal degradation i.e., becoming a thermoset material.

3.2.1 Crosslinking

Cross-linking is one of the ways in which a number of polymeric products are made for different purposes. Crosslinking improves the stability and performance of the material at high temperatures. E.g., Thomas et al. (2021) mention that crosslinked polyethylene plastics (XLPE) are a great material for electrical insulation in wire and cable coatings or hot water tubing. Vulcanization is also a method for forming crosslinks commonly used in hardening rubbers or rubber tires with sulphur. Zhao et al. (2018) have reviewed recent advances in utilizing vulcanization crosslinking to produce sulphur-containing polymers to replace elemental sulphur used as cathode active material in Li-S batteries. They conclude that this method “has become one of the most effective strategies to improve the cycle life of Li–S batteries.”

There are many physical and chemical types of crosslinking methods, but for lignin, the TO treatment, which is an initial process step used in the production of CF precursors, is seen as most suitable. Novel precursor for CF are PAN fibers, other less commonly known CF precursors are regenerated cellulose (rayon) and petroleum-based pitch, which is the most similar to lignin properties. Yuan et al. (2017) studied stabilization of mesophase pitch-based

fibers at different temperatures and processing times and examined the performance of the final product after carbonization and graphitization. Yuan et al (2017) also describe the TO treatment to be the most time-consuming and not really efficient process, which however, is a very important step to determine physical properties, i.e., quality, of the resulting CF. “Only a completely stabilized pitch fiber can be subsequently carbonized and graphitized without its structure melting, softening, relaxing or deforming.”

TO of lignin is a complex process and has not been well characterized. Several studies however, have been concluded about lignin-based CF precursors, since it has been estimated that low-cost lignin would save around 37–49% in the final production cost of CF compared to PAN precursors (Bajpai, P. 2017). For this thesis, the most relevant lignin-based CF studies were from e.g., Braun et al. (2005), who studied thermostabilization (TO) of lignin fibers in the presence of air and temperatures up to 340°C at various heating rates, from Cho et al. (2019), who studied the effects of TO treatment conditions of softwood kraft lignin on the resulting carbon structure of CF mats, and from Brodin et al. (2012), who investigated different purified kraft lignins in the TO treatment.

3.2.2 Glass-transition temperature T_g

One of the key things to consider among the changes in the properties of cross-linked polymers is the glass-transition temperature (T_g). Amorphous polymers, like lignin, will have properties similar to glass (strong and brittle) when below T_g, where bonds do not have the sufficient energy to move i.e., bonds have very little segmental motion (Engineers Academy, 2018).

Above the T_g these properties change. Lignin has a relatively high T_g, but well below carbonisation temperatures depending on the raw material and extraction method. E.g., for kraft lignin T_g usually varies between 124-174 °C and for Organosolv lignin between 91-97 °C (Bhattacharyya et al. 2020).

Factors affecting the T_g are e.g., molecular weight (higher degree of polymerization means longer molecular chains and higher Tg), degree of initial cross-links in the raw material, inter-molecular forces, chain branching and flexibility (PolymerWorld, 2019)

The aim in the TO treatment is to increase the T_g of lignin, which can be increased due to crosslinking and conjunction of oxidized groups. Crosslinked material has macromolecules joined to other macromolecules through covalent bonding, which are formed by removal of peripheral small groups (intermolecular bonds) from the polycyclic aromatic molecules and the insertion of bridging groups containing oxygen. In the case of lignin, heat treatment leads to homolytic cleavage (depolymerization) of alkyl-aryl ether bonds, like β-O-4 linkages and the formation (polymerization) of links between the aromatic benzene ring and neighbouring aliphatic chain, as seen in Figure 6 (Yuan et al., 2017).

The TO treatment also needs oxygen-rich environment, which aims to introduce additional oxygen into the compound. The rate and degree of cross-linking is linked to the amount of free oxygen. Poletto (2018) state that the using strong oxidants break up the aromatic ring of the polymer, but using milder ones, like air, changes only its functional groups. The lignin contains many hydroxyl groups, which can be oxidized to carbonyl groups, and these functional groups are more reactive than the hydroxyl groups.

Hasan et al. (2020) studied blending lignin with other polymers, like polypropylene, and discovered than "the more phenolic hydroxyl in lignin, the more free radicals could be trapped, which was beneficial to the thermal oxidative stability of polymer samples." Which might be the case too for the TO treatment of pure lignin.

As a result of oxygen introduction to the TO treatment, elemental analysis is an effective way to study the effect of the TO treatment, although elemental analysis cannot reveal information on the structure of the products of the reaction. Braun et al. (2005) reported that the O% increased up to 250 °C and decreased after this point, whereas Cho et al. (2019) discovered, that the O% increased up to 350 °C in the TO treatment in their study.

The formation of carbonyl groups is accompanied by the evolution of lower molecular weight products such as H_2O, CO, CO_2, etc. as seen in Figure 6. Therefore, a change in mass and variation in the proportions of oxygen and other elements occur simultaneously during the TO treatment (Yuan et al., 2017).

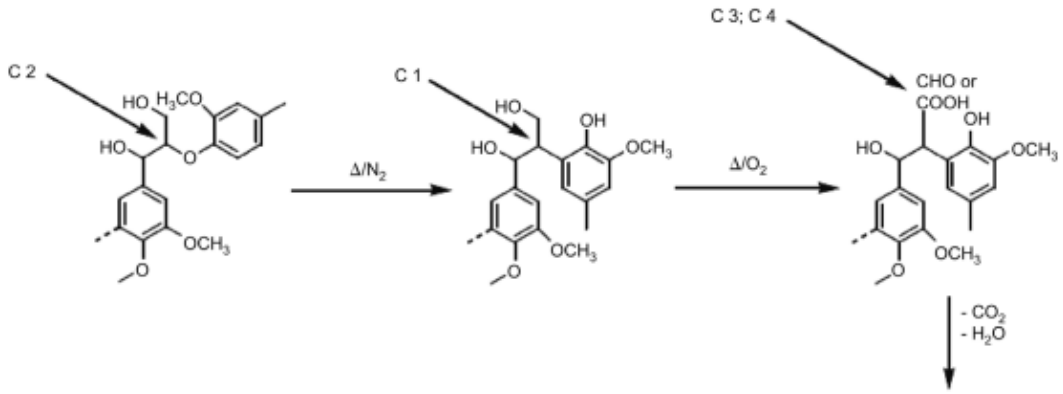

Figure 6. cleavage of β-O-4 and formation of linkage between aromatic ring and aliphatic chain (Brodin et al. 2012)

As cross-linking goes on, we end up with high T_g, which means a strong covalently bonded network in the material and glass-like state at higher temperatures i.e., with a thermoset material. To prevent lignin from melting in the TO treatment, a slow heating rate is paramount. in keeping cross-linking reactions happening faster as temperature rises.

4 Design of experiments

The design of experiments (DOE) methodology refers to the use of statistical tools and techniques to increase the understanding of a process and to determine how controlled and uncontrolled factors are related to process outputs, while keeping the number of required experiments / tests at a minimum. It is used in various applications to e.g., determine which factors have a significant effect of a response, identifying the effect on interactions between two variables or optimizing process performance (Jiju A. 2023)

4.1 Research layout

The DOE started with choosing the key factors and the right DOE method. For this study, three key factors were identified and based on those a full-factorial design with a center point was chosen as a DOE method. The factors are presented in Table 2. the key factors are run

in each possible combinations for low and high values and at a center point trial with process parameters between the low and high values.

Process parameter (Factor)	Unit	Low	Centre	High
Max. temperature	°C	T1	T2	T3
Holding time	h	t1	t2	t3
Heating rate	°C/min	k1	k2	k3

Table 2. DOE factors

Literature references were used to set the basis for the DOE key factors and parameter values. Cho et al. (2019) studied the effects of TO treatment conditions on the resulting carbon structure of CF mats and created a two-level factorial design for optimization of parameters. Brodin et al. (2012) had also made a similar experimental design for birch lignin powder, mix of spruce and pine lignin and lignin fibers. Du et al. (2021) studied the pre-oxidation mechanism of lignin precursors for hard carbon anode to enhance performance. Another relevant study Braun et al. (2005) was mentioned above.

Exact process parameters are not shown here for company IPR. The low and high values were decided based on existing knowledge.

The DOE project was started in Minitab software, where we chose to include the center point and repetitions for two corner points and the center point to verify the test results. Later in the middle of the trial runs, a repetition of two additional corner point was decided (RO 13 and 14). In total that makes 2^3 + center point + repetitions = 14 trial runs. A randomized order to conduct the trials was created by the software, as can be seen in Table 3. Some manual modification was done to the order, however, the trial with highest temperature and holding time was moved first to see if the resulting lignin had melted and if there was a need to lower the T3 temperature. Also, the repetitions of the corner points were moved to the end of the order list for time-related issues with the experiments.

Run order (RO)	Run nro.	Max. temperature (MT)	Holding time at max. temperature (HT)	Heating rate (HR)	Repetition
1	8	T3	t3	k3	
2	10	T2	t2	k2	
3	7	T1	t3	k3	
4	4	T3	t3	k1	
5	1	T1	t1	k1	
6	3	T1	t3	k1	
7	9	T2	t2	k2	x
8	6	T3	t1	k3	
9	2	T3	t1	k1	
10	5	T1	t1	k3	
11	11	T3	t1	k1	x
12	12	T1	t3	k3	x
13	13	T1	t1	k1	x
14	14	T3	t3	k3	x

Table 3. Experimental design with chosen factors

Figure 7 shows a geometric illustration of the used 2^3 factorial design with factors. Red dots present high and low points of the factors and the blue dot is the center point. Yellow dots on the red and blue dots present a repetition point.

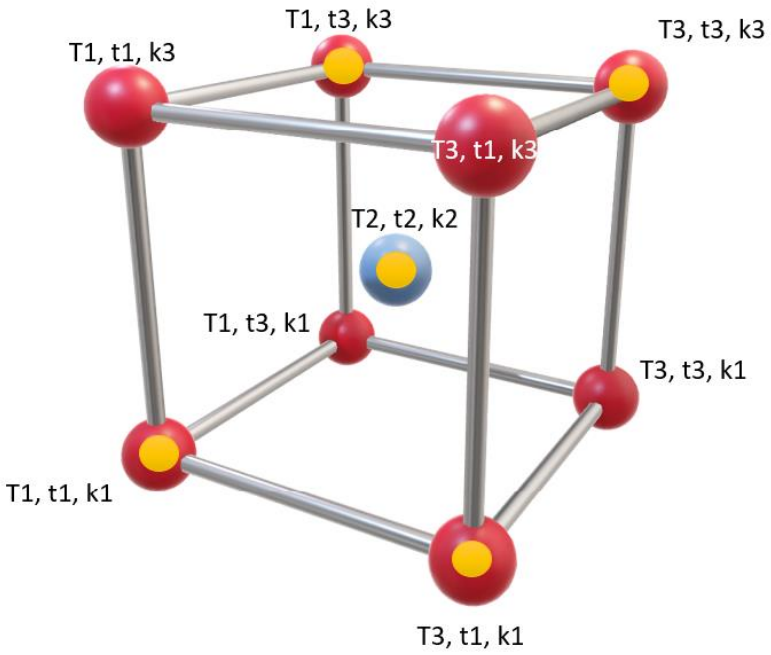

Figure 7. 3D illustration of the factorial design

4.2 Equipment and materials

The trials were performed with a lab-sized batch kiln at Stora Enso facilities. 100g of raw material were loaded into the kiln and test were run according to Table 3. The kiln atmosphere was air and the kiln was equipped with a blower to circulate the air. The kiln was programmed to heat first to 130 °C at the heating rate of 2 °C/min to dry the raw material. After 30 minutes the next step was programmed according to the factors. After the heating program, cooling started by letting the kiln cooldown naturally without the blower. The heating curve is visualized in Figure 8. Due to time related issues, the trials were conducted with two similar batch kilns. One repetition was made to see if there's any difference in the analysis results between kilns, this repetition is the RO 13.

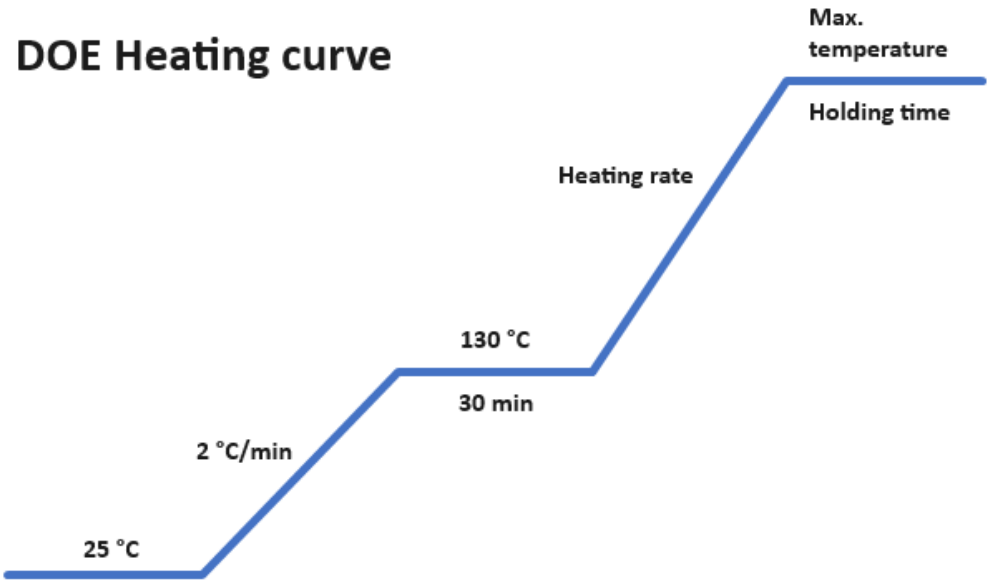

Figure 8. Heating program curve

The raw material used for this study is standard softwood kraft lignin produced at Stora Enso's Sunila mill. The lignin is separated from black liquor with Valmet Lignoboost® technology. All raw material was from the same source and batch, and one reference sample was taken from the batch. The same analyses were performed for the reference sample. The raw material was mixed before dividing it for each trial for two crucibles containing 50g material each. Two crucibles were chosen instead of one was chosen for a better fit in the kiln.

After the kiln had cooled down under 50 °C, the sample was removed from the kiln and stored in a closed sample container.

4.3 Analytical methods & sample preparation

4.3.1 OEA

Organic elemental analysis (OEA) is used to measure the total C, H, N, S and O in the material. A flash 2000 elemental analyzer was used for the analysis of these elements of the samples. A standard operating procedure based on the operating manual was used for sample preparation, analysis and reporting. The oxygen (O) content was measured separately from

the other elements, since measuring oxygen requires the use of another furnace and different sample preparation. Calibration of the equipment was done before both C, H, N, S and O measurements. For the calibration of C, H, N, S, the samples were first dried at 105 °C for 1 hour and then a few milligrams of the sample were weighed into tin crucible with vanadiumpentoxide for the detection of sulphur. For the analysis of oxygen, silver crucibles were used and vanadiumpentoxide was not needed. Three replicates for each sample were prepared and the average content of each organic element was calculated by the Flash 2000 software.

4.3.2 XRF

X-ray Fluorescence (XRF) has limitations to what elements can be measured; it cannot be used to measure elements that are lighter than magnesium thus not being able to measure carbon (Thermo Fisher Scientific, 2020). The XRF spectrometer method was used for TO-treated lignin to identify elements like Na, Al, Si, S, K, Ca, V, Cr, Mn, Fe, Ni, Cu, Mo and Ba with Wintrace, an analytical software. Three replicates of XRF samples were prepared and analysed in helium atmosphere. Al, Si, S, Ca and Fe were considered most relevant elements. If these elements were increased, contamination from kiln or preparation methods had happened. Contamination could affect the analysis results and lead to outliers or wrong conclusions from the analysis data. Uniquant, a standardless, semi-quantitative software measurement for fast screening of unknown samples was used to identify all elements in raw material before TO treatment.

4.3.3 DSC

For the determination of the T_g of lignin and TO-treated lignin, a Modulated Differential Scanning Calorimeter (MDSC) Q2000 system was used. A standard test method for sample preparation, calculation settings and reporting was applied.

Differential Scanning Calorimetry (DSC) measures the temperature and heat flows associated with transitions in materials as a function of time or temperature. Material properties such as T_g, melting temperature, crystallization energy, specific heat capacity, curing behaviour, purity, and thermal stability can be measured via DSC. T_g is the

temperature range at which an amorphous polymer changes from a hard/glassy state to a soft/leathery state, or vice versa. Traditional DSC provides a single signal which is the sum of all thermal events occurring at a specific temperature which causes difficulties to identify small transitions.

MDSC improves upon traditional DSC since it can be used to see a small transition in samples, as MDSC is a technique which offers advantages in sensitivity, resolution and separation of overlapping transitions. MDSC measures the total heat flow, and additionally heat capacity component (reversing heat flow) and obtains the kinetic component (non-reversing heat flow) from their difference. In calculation, kinetic events (e.g., water evaporation and enthalpic recovery) are separated from the changes in heat capacity (e.g., the T_g).

Figure 9. shows the heat flows measured with MDSC. From the total heat flow, which is the only heat flow measured with DSC, we cannot see the T_g at all, or not accurately enough. Reversing heat flow shows the T_g more accurately if there is one to be found.

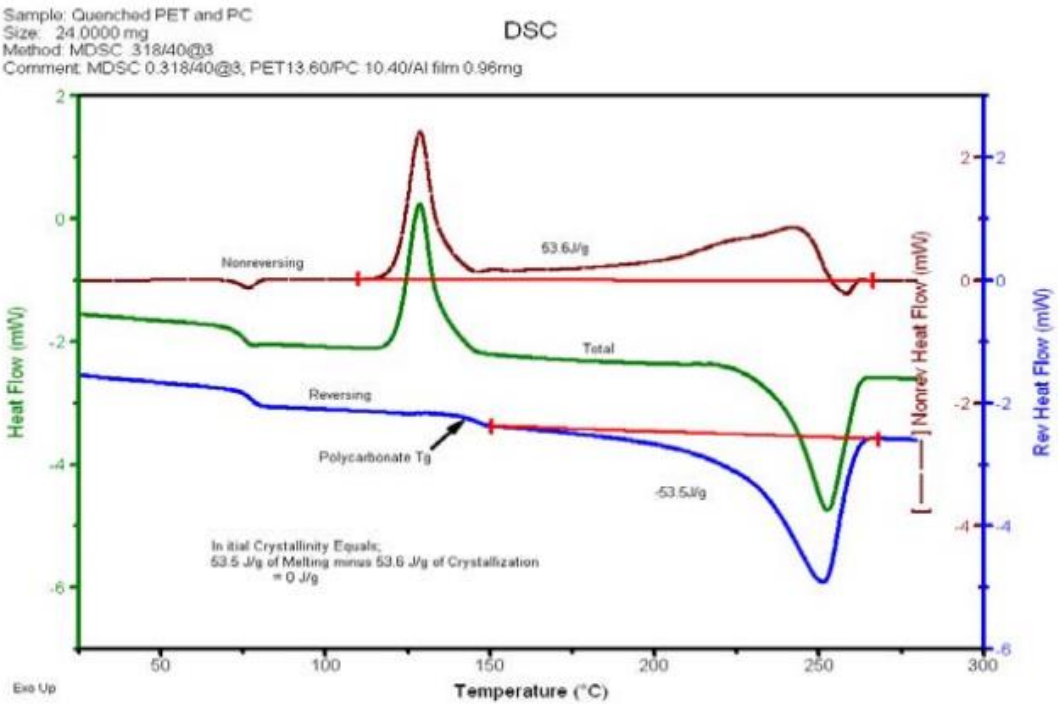

Figure 9. Example of MDSC data (TA Instruments, 2005)

The temperature of a sample in MDSC changes sinusoidally. “The resulting heat flow is a function of the rate of temperature change, absolute temperature, sample mass and the specific heat of the sample (TA Instruments, 2007).”

$$\frac{dH}{dt} = Cp\frac{dT}{dt} + f(T,t)$$

Where:

$\frac{dH}{dt}$ = Heat Flow Rate (mW or W/g)

Cp = Sample Specific Heat (J/g°C) x Sample Mass (g)

$\frac{dT}{dt}$ = Heating Rate

$f(T,t)$ = Heat Flow Rate due to Kinetic Processes (mW or W/g)

Few milligrams of the sample are prepared and weighed into tin crucibles. A small hole is cut into the lid of the tin crucible with a needle to remove the evaporated gas. Two replicates were done from all samples, except for the first one with three replicates to confirm variability. The samples were placed into the autosampler of the Q2000 device and the measurement started. The start and end peaks for the T_g curve were selected manually in the resulting graph, and the T_g value automatically calculated.

4.3.4 TGA

A thermogravimetric analysis TGA Q500 system was used for thermal analysis of the samples. TGA measures the rate of weight change and amount in a material isothermally as a function of time or as a function of increasing temperature, in a controlled atmosphere. “It can be used to characterize any material that exhibits a weight change and to detect phase changes due to decomposition, oxidation, or dehydration. This information helps to identify the relative weight change and correlate chemical structure, processing, and end-use performance (TA Instruments, 2006).”

TGA was used to obtain the yield after TO treatment and carbonisation at 1000 °C at a heating rate of 10 °C/min. The yield was calculated by the TGA software. The sample was

first dried for 100 minutes and then the weight was reset to the present weight of the 100 % dry lignin, where the remaining yield was compared.

Few milligrams of the sample are prepared on a pan. As in DSC, two replicates from all samples, except for the first sample with three replicates. The samples were placed in the autosampler, and the analysis run started.

4.3.5 Yield after TO treatment

The lignin weight was checked before and after TO treatment with an analytical scale depicting an accuracy of 0.01 grams to track the total mass loss. Empty crucible was tared and 50 grams of material was added. The sum of two crucibles were s

5 Results and discussion

The DOE study consists of 14 sample points total and analysis of organic elements (OEA) and XRF for other elements, carbonization yield at 1000 °C, MDSC for examining the glass-transition temperature and reaction energy. Analysis of the factorial designs for was done with Minitab, and Appendices 2 – 7 contain model summary, variance analysis, regression equation, pareto chart and normal probability plot for T_g, reaction energy, carbonization yield, TO treatment yield, C% and O%. These results are presented in detail below. Versus fits and versus order charts were left out but will be discussed if any abnormalities were found. Other analysis results, e.g., not as relevant measured elements, are discussed more shortly.

In factorial analysis, all regression models used the confidence level $\alpha = 0.05$. This means that the chance of concluding that the model fits the data is 95 %. The pareto chart shows which terms contribute the most to the variability in the response. A reference line indicates the significance level. Any bar extending beyond the line is a significant effect. Factorial regression models were reduced i.e., insignificant factors removed up to point, where only significant factors remained. Some exceptions were made but will be discussed later. The

Pareto chart shows significant factors and the normal probability plot shows that the residuals follow a normal distribution.

Another key results to pay attention from factorial regression, is P-value, which shows the significance of each factor. The P-value should be smaller than $\alpha = 0.05$. A lack-of-fit P-value, however, is smaller than $\alpha = 0.05$ when the model does not fit the data, so we want P-value to be higher than $\alpha = 0.05$. The model summary tells us how well the model fits the data. The higher the R^2 value, the better the model fits your data. The predicted R^2 determines how well your model predicts the response for new observations. Models that have larger predicted R^2 (pred) values have better predictive ability (Statistical Modeling, n.d.)

Residual vs. fitted chart, and residual vs. order chart were left out from appendices. Formerly mentioned show a random spread, i.e., constant variance of the residuals, major outliers are not preferred, and the latter, residuals vs order plot shows that the residuals are randomly scattered around zero in the optimal case

Table 4 shows the results for significant analysis, T_g, reaction energy, carbonization yield, yield after TO treatment, C% and O%. The color of the row represents a repetition point. The results displayed are the mean values from two or three replicated, depending on the analysis. The analysis of the raw material are not presented separately, but will be compared and discussed with each analysis in question.

Run order (RO)	Max. temperature	Holding time at max. temperature	Heating rate (HR)	Repetition	MDSC		OEA		TGA	Mass loss after TO treatment
	(MT)	(HT)			Tg (°C)	Reaction energy (J/g)	C %	O %	Yield %	Yield %
1	T3	t3	k3		n/d	n/d	70,0	22,4	46,6	85,9
2	T2	t2	k2		n/d	n/d	69,1	22,7	46,1	88,3
3	T1	t3	k3		185,6	1,20	68,9	22,4	44,4	88,8
4	T3	t3	k1		n/d	n/d	70,2	22,3	51,2	85,1
5	T1	t1	k1		175,5	1,11	68,7	23,2	42,1	90,6
6	T1	t3	k1		185,2	0,89	69,2	23,2	46,0	89,5
7	T2	t2	k2	x	189,6	0,84	69,0	22,8	45,3	87,3
8	T3	t1	k3		184,8	1,63	69,2	22,5	42,6	86,9
9	T3	t1	k1		n/d	0,50	69,2	22,7	46,4	87,0
10	T1	t1	k3		173,6	1,25	68,4	23,2	39,3	91,1
11	T3	t1	k1	x	n/d	0,55	69,2	22,4	47,8	87,0
12	T1	t3	k3	x	189,0	1,08	68,2	23,3	45,0	89,1
13	T1	t1	k1	x	172,9	0,99	68,2	23,3	42,0	n/a
14	T3	t3	k3	x	n/d	n/d	69,2	22,7	47,6	n/a

Table 4. Analysis results

5.1 MDSC

5.1.1 Glass-transition temperature

The MDSC results show that the T_g value increases up to a point, before reaching a value of approximately 190 °C and then disappears. This is seen as a point, where lignin is fully cross-linked and should be considered a target value. After this point, further TO reactions do not happen, i.e., processing is complete. Table 4 shows the T_g value n/d (not detected) for these samples. Appendix 1 shows the example of a MDSC data graph from RO 1 and RO 13 where the first mentioned does not have a T_g and the latter one has. For RO 1 the reversing heat flow (blue line) shows a linear trend and no T_g. For RO 13 the reversing head flow shoes a step-like curve (T_g) and the non-reversing heat flow shows that kinetic reactions, i.e., crosslinking or other reactions, are still happening.

For RO 9, one replicate sample had a T_g, but was considered an outlier and excluded from the results. RO 11 was a repetition point of RO 9. MDSC analysis of both samples were almost identical, except the one replicate with the T_g. which gave more certainty that is was an outlier.

Surprisingly, for the first run of the center point (RO 2) T_g was not obtained, but the repetition of the center point (RO 7) had a T_g value of 189.6 °C, which is very close to our target. This could indicate that temperature T2 would be optimal when considering only the T_g value. The T_g was lost in all runs at temperature T3, except for one point (RO 8), which is probably a result of fastest overall processing time from combination of fast HR and short HT. RO 8 was also considered an outlier in the factorial regression charts.

Figure 10 shows a bubble plot of T_g, with MT on the x-axis, HR as bubble color and HT as bubble size. From this we can determine that a higher MT with a higher HT result in a higher T_g. At T1, the top two green big bubbles (RO 3 & 12) and the bottom blue small bubbles (RO 5 & 13) are repetitions and are very close to each other, indicating good reproducibility.

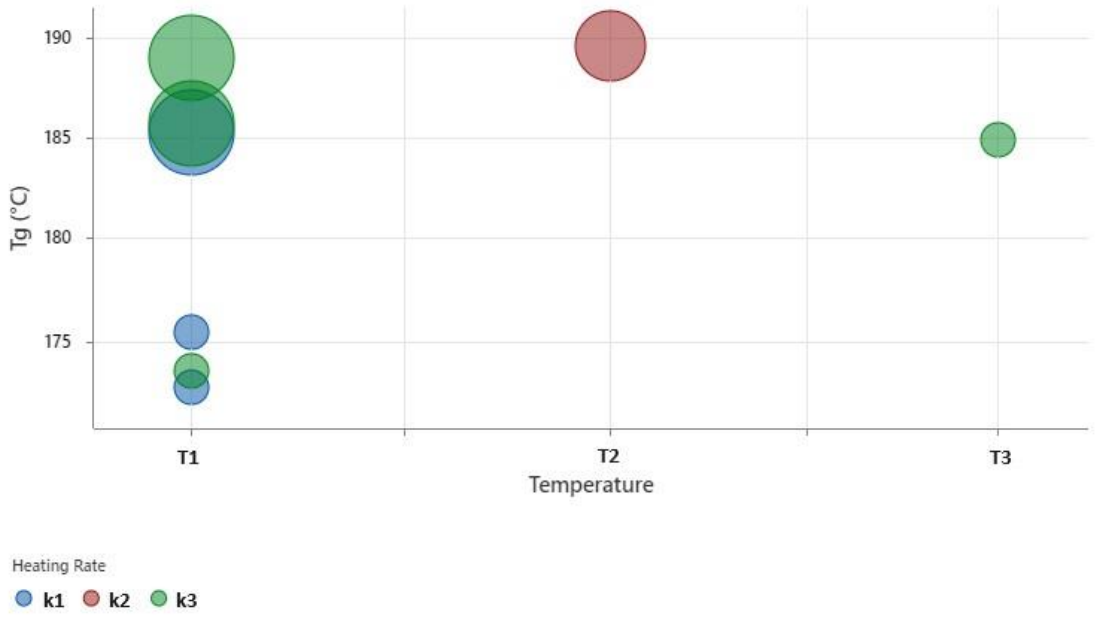

Figure 10. bubble plot of T_g

The Pareto chart in Appendix 2 shows that significant factors for T_g seem to be MT and HT and the model summary R^2 value of 93.0 % shows that the model fits the data quite well. The predicted R^2 is 69.5 %. The T_g model was done with the 8 samples, where the T_g was obtained. The main effects of MT and HT are seen in Figure 11.

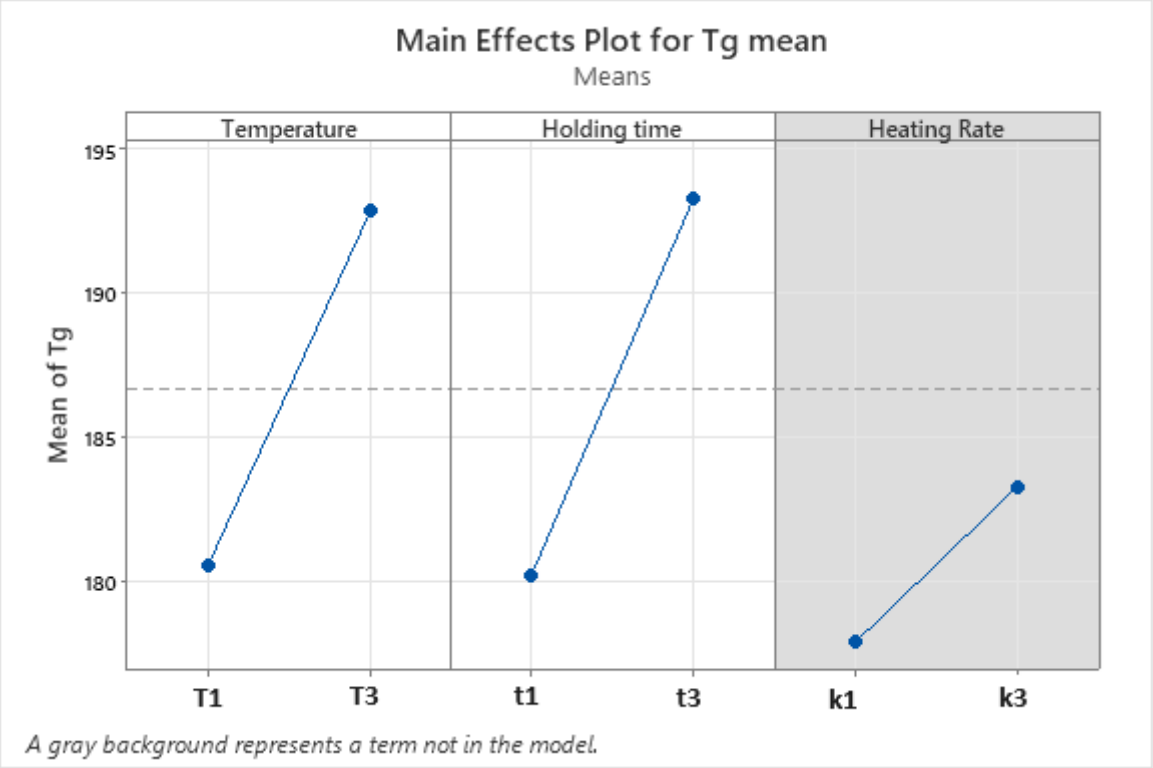

Figure 11. Main effect for the Tg

5.1.2 Reaction energy heat flow

MDSC measurements also shows the kinetic component (e.g., reaction energy) as non-reversing energy. In case of lignin, this means water evaporation at lower temperatures and after reaching 130 °C, hypothetically reactions related to crosslinking, decomposition, vaporization of CO, CO_2, etc. This can be also seen in Appendix 1, where RO1 does not have kinetic energy after water evaporation, but RO 13 has a small peak in the same temperature range as the T_g. It was found that two measured test runs had kinetic energy in the same temperature range, but T_g was not obtained, these are RO 9 and RO 11, which are also repetitions.

Appendix 6 shows the factorial regression for the reaction energy. Only HR and MT*HR were found to be significant, although the MT and HT were left in the model, MT because of MT*HR interaction and HT because model did not give a predicted R^2 value without it. The R^2 value is 94.7 %, and the predicted R^2 is 21,2 %. Figure 12 shows the main effects plot for reaction energy, where HR has a very significant effect on the reaction energy.

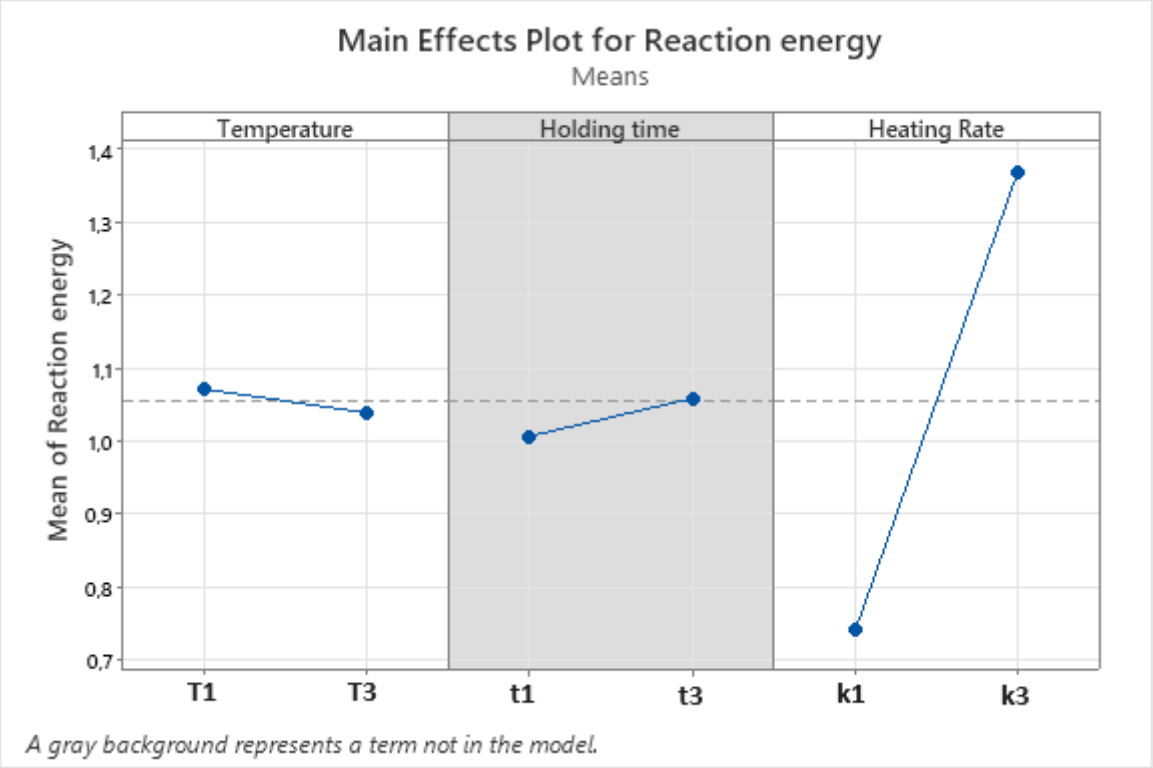

Figure 12. Main effect plots for reaction energy

Similarity of repetitions was also checked, and the only distinct difference was noticed in the center point, RO 2 and RO 7. It was estimated that that kinetic component should reach 0 to be fully cross-linked i.e., fully processed. The center point (RO 2) does not have neither T_g or reaction energy in any replicates, but repetition point (RO 7) has a T_g value and reaction energy in all replicates. Lowest reaction energy measured was 0.48 J/g in one replicate of the RO 9, but RO 7 had one replicate a reaction energy of 0.76 J/g.

Much can be speculated from this result, either RO 2 or RO 7 is an outlier, reaction energy measurement is not accurate, or that other anonymous factors or correlations are at play. In any case, more data in needed to verify the significance of reaction energy.

5.2 Elemental analysis

Factorial regression was done for the oxygen (O%) and carbon (C%) contents, as these were seen as most relevant for this study. Other elements, like H, N and S measured by OEA and the elements measured by XRF are discussed shortly at the end of this chapter.

5.2.1 Carbon content C%

For the C%, MT and HT were significant factors in the factorial design. In Appendix 4 we see that the R^2 value is 76.6 % and the predicted R^2 is 51.5 %. Factor C (HR) was left in the model, however not counting as significant factor, because the model accuracy increased and R^2 value raised by 6 %. Versus charts did not show any major outliers. It was an expected result that C% increases in higher MT and longer HT. Figure 13 shows the main effects plot for C%.

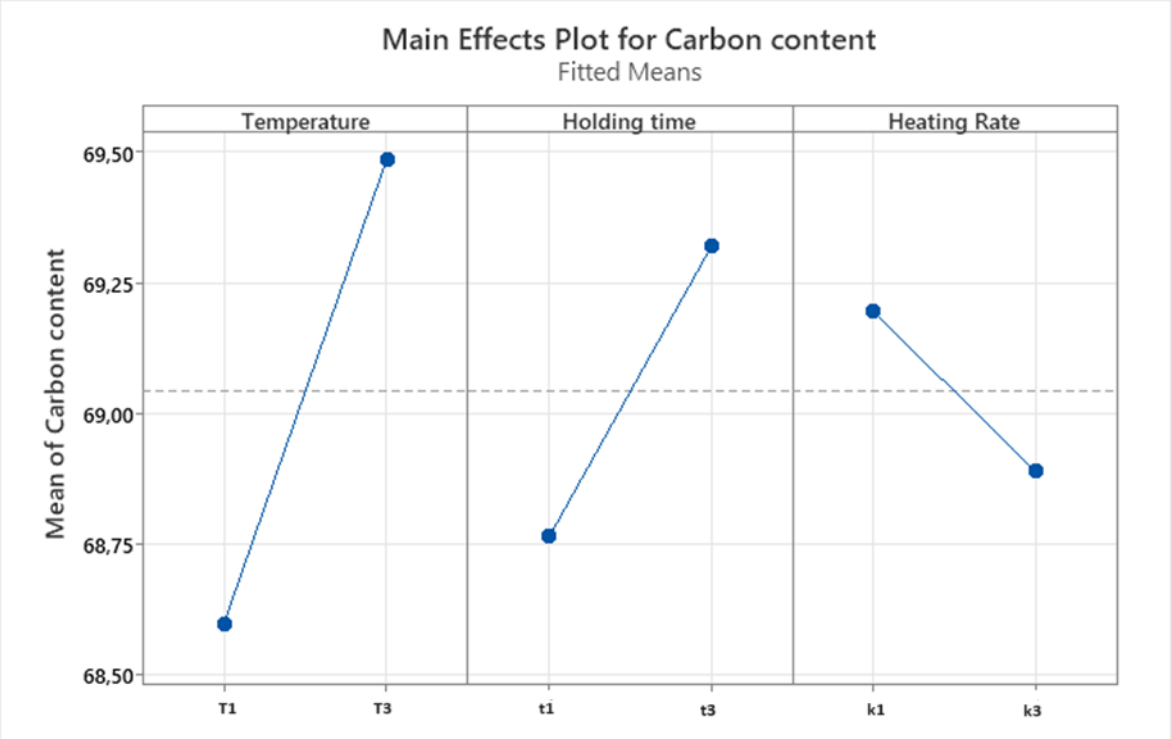

Figure 13. Main effects for the C%

5.2.2 Oxygen content O%

For the O% factorial regression it was a challenge to choose the significant factors and the most fitting model. In every scenario some correlation was decreasing as another one increased. I ended up with a model shown in Appendix 5, which shows the MT factor as only significant one. HT factor was also included since predicted R^2 value increased greatly with it. R^2 value of 65.8 % and a predicted R^2 value of 41.25 % was obtained. Reducing the model to only MT as significant factor gave a R^2 value of 52.6 % and a predicted R^2 30.9 %. Figure 14 shows the main effects plot of the model.

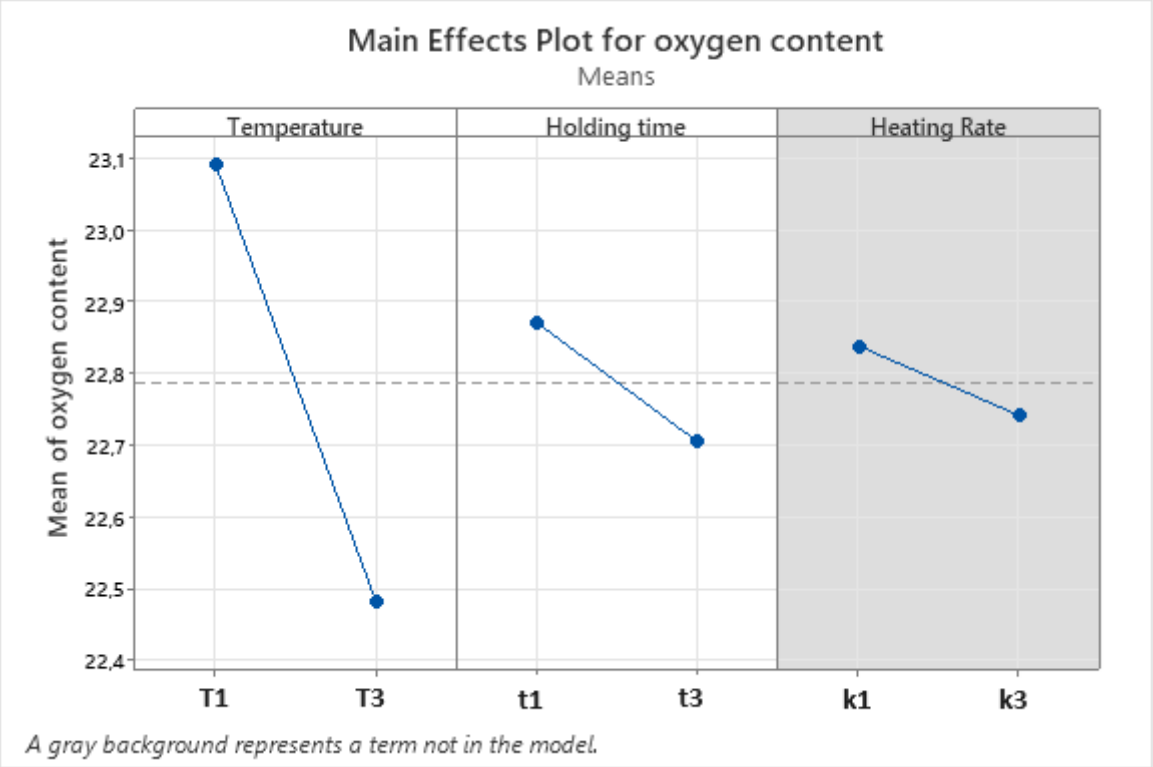

Figure 14. Main effects plot for the O%

Oxygen content analysis revealed that O% correlated most with the temperature and that O% decreases as the temperature rises. This observation aligns with the results discovered by Braun et al. (2005). Based on their study, it is expected that the O% increases to a maximum and then decreases with increasing temperature, reflecting the uptake of oxygen during cross-linking and/or loss of carbon at lower temperature, and increasing loss of oxygen and

(less of) carbon during decomposition at higher temperature The raw material had an O% of 24.8 %, so after reaching T1, O% had already decreased by 2-3 %.

One replicate of RO 3 oxygen measurement had considerably smaller value and thus standard deviation four times larger. Removal of the outlier made the model much more fitting also in this case. The R^2 value increased to 89.8 % and the predicted R^2 to 85.6 %, with MT as only significant factor. The variance was also improved. Although the model fits the data better without the outlier, significant factors are not much affected. Original model in Appendix 5 was still chosen as more fitting.

Figure 15 shows the mean O% decrease as temperature increases.

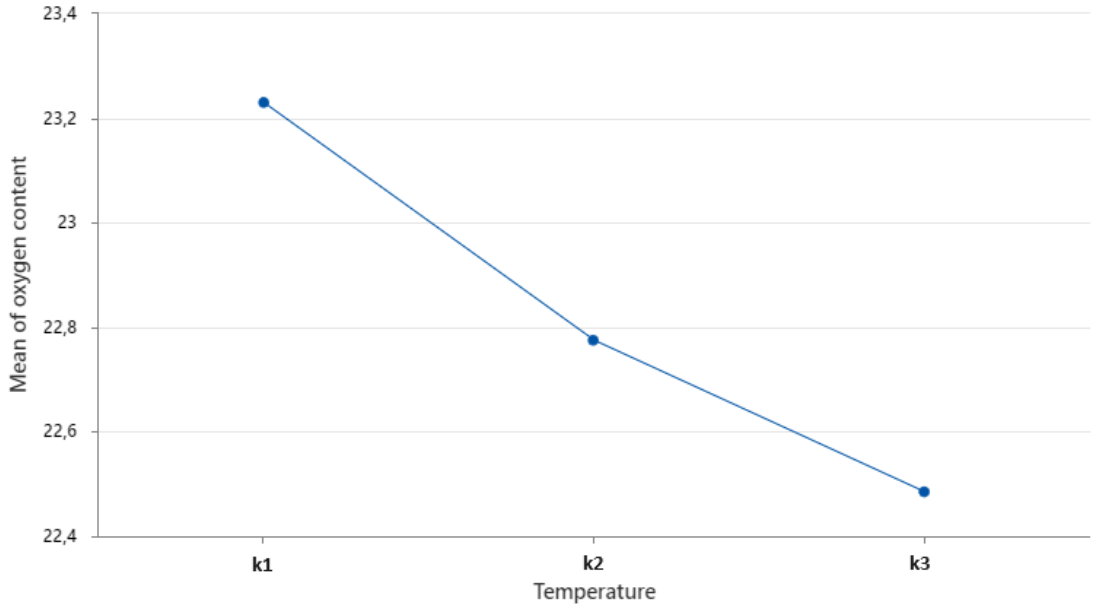

Figure 15. mean O% decrease with temperature increase

5.2.3 Other elements

OEA analysis also measured H, N and S elements. From these no regression models were made. Hydrogen (H) decreases marginally with higher MT, longer HT and faster HR. Nitrogen (N) stays the same, or increases very slightly. Both XRF and OEA gave results for the sulphur content of the sample, from these, the OEA result was seen as more accurate based on previous experience at Stora Enso. Sulphur (S) decreases slightly with both MT

and HT. All these changes are probably due to variation in the proportions of elements occurring during the TO treatment.

XRF results did not show that any contamination had occurred during the sample processing in any test runs. All elements, mostly Al, Si, Fe, increased only slightly, probably because of mass loss (C, H and O elements). With XRF the sulphur content was measured from both the raw material and TO-treated lignin. From these we can roughly estimate that the sulphur content decreased during the TO treatment by approx. 50 – 63 %. However, XRF measurements are not considered as accurate as OEA.

5.3 TGA

Appendix 3 shows the factorial regression for carbonization yield measured with TGA. This model fits the data most accurately from all five models with a R^2 value at 97.6 % and a predicted R^2 at 92.7 %. Versus charts show good variance but the lack-of-fit is not as high as in other models. Lower lack-of-fit is not, however, seen to have any effect. The significant factors are surprisingly many and most significant are HT, MT, HR and the MT*HR interaction. The main effects plot (Figure 16), shows that higher MT, longer HT and slower HR all have significant effect on the carbonization yield after carbonization at 1000 °C.

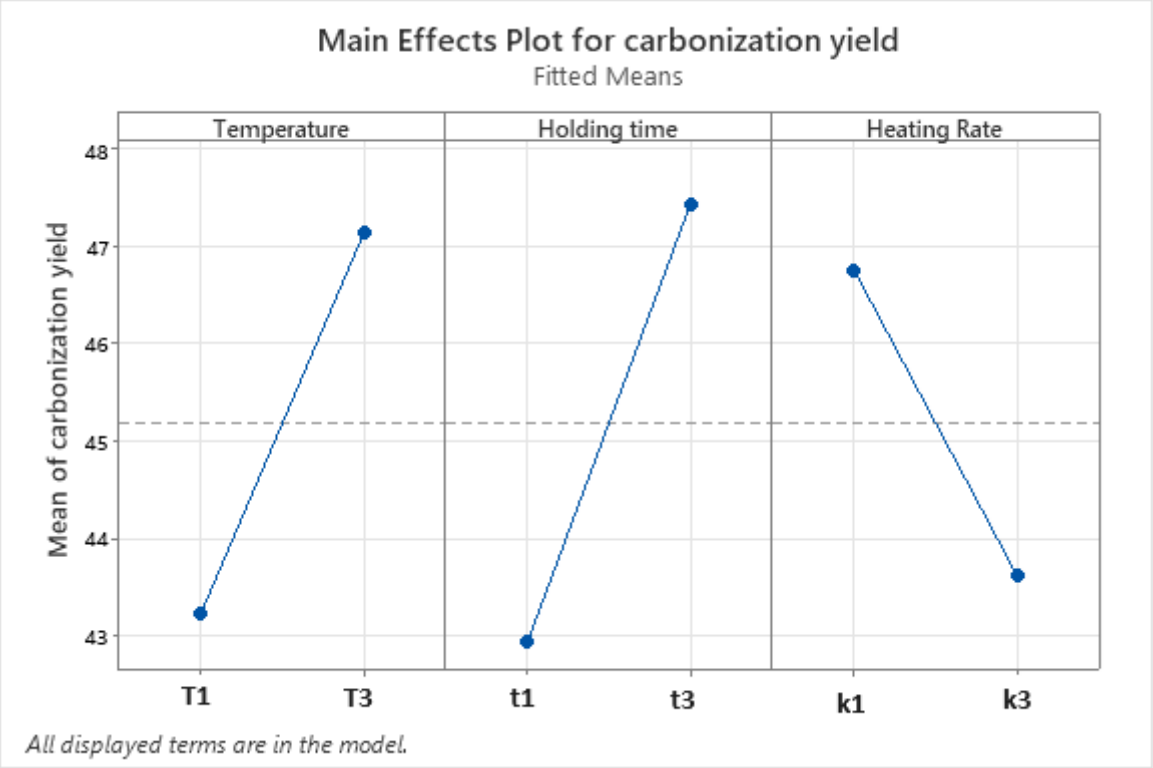

Figure 16. Carbonization yield main effects plot

5.4 TO treatment yield

Factorial regression for yield after TO treatment is seen in Appendix 7. R^2 value of 97.03 % and predicted R^2 value of 95.47 % shows a good fit of the data. No major outliers are noticed. Table 4 shows that RO 13 and RO 14 result for TO treatment yield is not available. This is because RO 1 and RO 13 both were processes with only 50 grams and the sum of these was used to present RO 1. RO 14 is missing due to operational error.

Figure 17 shows the main effects to be MT and HT and that highest TO yield is achieved in lower MT. This result seems excepted at first since mass loss accelerates in higher temperatures. On the other hand, higher MT also seems to result to higher carbonization yield.

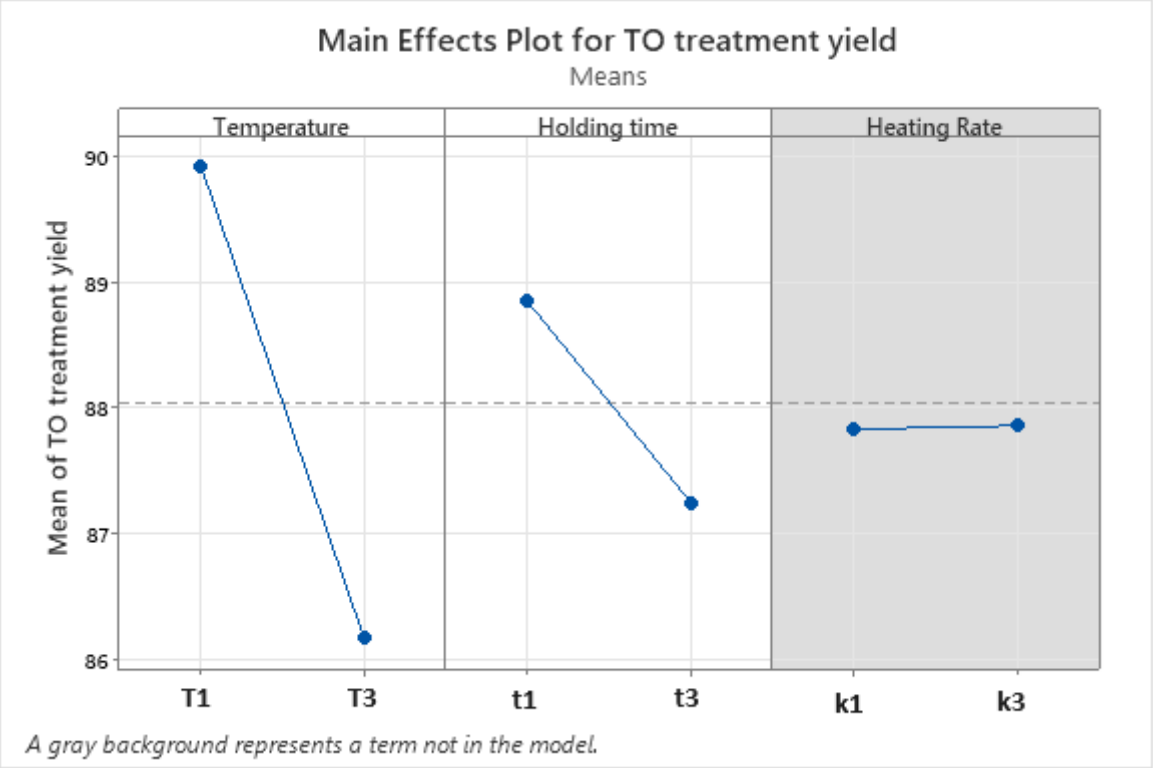

Figure 17. The main effects for TO treatment yield

5.5 Optimal process parameters

The last research question presented in the introduction chapter was to determine optimal key parameter settings to produce well performing oxidized lignin with minimal time. As we can conclude from the analysis results, MT remains as a significant factor in all results and HT as well, except for the O% and the reaction energy. HR has a great effect on reaction energy, and a smaller effect is seen for carbonization yield and C%. Figure 18. summarises the behaviour of factorial regression models as surface plots. C% was left out, as it is almost identical to the carbonization yield surface plot. Also, O% was not seen as relevant to present. The third variable (HT in reaction energy and HR for others) was kept constant at the center point (t2, k2).

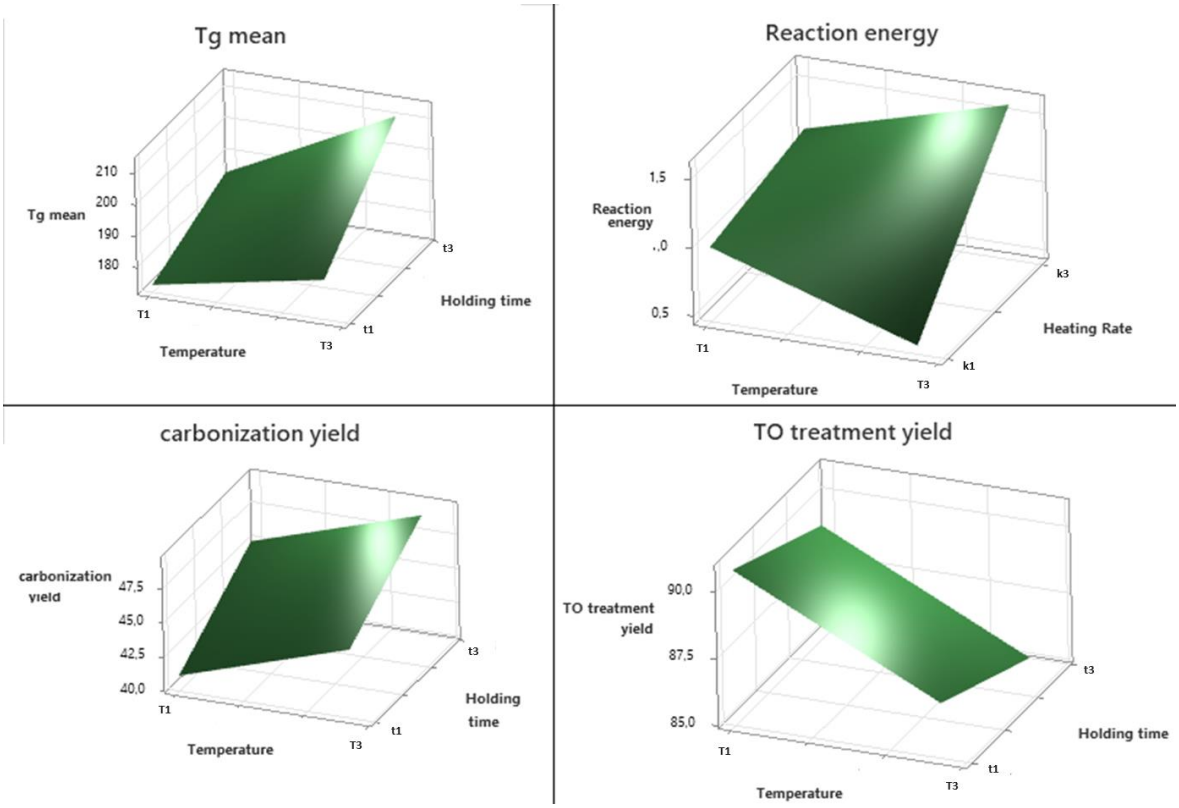

Figure 18. Surface plots for responses versus their significant factors

Minitab software can be used to optimize the chosen responses to reach a certain goal, to maximize or to minimize. There's also an option to set constraints for factors such as set HR for certain value or region.

To optimize the factors to produce well performing oxidized lignin, first it is needed to define and rank the importance of each output variable (analysis parameter, response). If fully oxidized lignin is the wanted outcome, we probably want to maximize the result for the T_g and minimize the reaction energy. These two analysis parameters are seen to affect the quality. As secondary goal we want to have a cost-effective process, meaning maximizing the carbonization yield. To conclude, higher MT and HT and slower HR all have a positive effect on significant responses, T_g, reaction energy and carbonization yield.

In the settings it was decided to use goals to define wanted outcomes. For the T_g, goal was set to maximum of 190 °C, and upper value as 192 °C as we cannot determine the T_g value after this point. For reaction energy we determined a goal of 0.5 J/g. The reaction energy

measurement showed a lot of deviation between samples, but not between replicates, so we set the upper limit for 1.1 J/g. The importance factor for both was set to 3, as they are seen as primary goals. For the carbonization yield the target was set to 50 % yield and importance as a value of 1.

Figure 19 shows the response optimization chart for the carbonization yield, reaction energy and T_g based on the definitions above. Optimal solution shows that with parameters [T3, t1+n, k1] we reach the T_g value of 190 °C, reaction energy of 0.51 J/g and carbonization yield of 47.64 %. HT factor at t1 + n means that optimal HT was optimized to between t1 and t2. Confidence interval (95% Cl) gives interval where you can be 95% sure current, calculated values fit. Predicted interval (95% PI) is the range of values where your calculation fits to predict future runs.

For the optimal parameters, a single outcome was a challenge due to a lack of the T_g and the reactions energy measurements of some samples. As a compromise, Figure 19 shows the optimal parameters from samples with reaction energy, reducing the data to 10 samples.

Response optimizations were also done for single responses to see if there was any major difference to Figure 19 results. The standard error fit (SE Fit) changed only marginally for T_g and reaction energy and more for carbonization yield. For single response, some factor parameters changed. There were no major changes, except when optimizing only carbonization yield. Maximizing or even increasing carbonization yield increased HT significantly, up to a point at t3 and carbonization yield of 51 % with [T3, k1].

Response optimization

Parameters

Response	Goal	Lower	Target	Upper	Weight	Importance
Tg	Target	187,000	190,0	192,0	1	3
Carbonization yield	Target	45,000	50,0	55,0	1	1
Reaction energy	Target	0,498	0,5	1,1	1	3

Solution

Solution	Temperature	Holding time	Heating Rate	Tg Fit	Carbonization yield Fit	Reaction energy Fit	Composite Desirability
1	**T3**	**t1 + n**	**k1**	190	47,6356	0,511103	0,905310

Multiple Response Prediction

Variable	Setting
Temperature	**T3**
Holding time	**T1 + n**
Heating Rate	**k1**

Response	Fit	SE Fit	95% CI	95% PI
Tg	190,00	1,20	(187,16; 192,84)	(184,08; 195,92)
Carbonization yield	47,636	0,414	(46,571; 48,701)	(45,752; 49,519)
Reaction energy	0,5111	0,0842	(0,3052; 0,7170)	(0,1448; 0,8774)

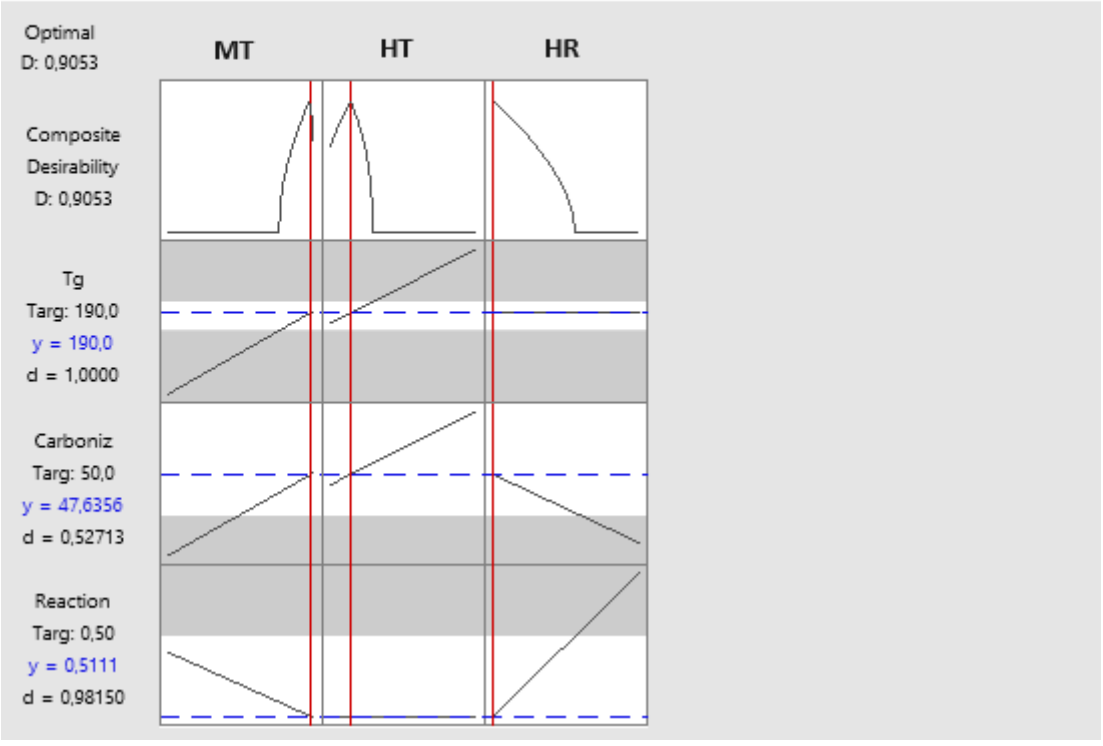

Figure 19. Response optimization of carbonization yield, reaction energy and Tg

Conclusions

This study corresponds well to the other studies conducted about TO treatment of lignin and complements the knowledge about lignin and its TO processing behaviour, e.g., Brodin et al. (2012) in many analysis results. In their study, the T_g was not detectable either for some samples. However, they did not consider the T_g model as significant as yield after TO treatment and yield after carbonization with the TGA. Both of their yield analysis also corresponds to the results of this study, the harsher conditions, high MT in combination with long HT and slow HR elevate the yield after carbonization, but after TO treatment, highest yield is achieved in lower MT. This can be seen in Figure 20.

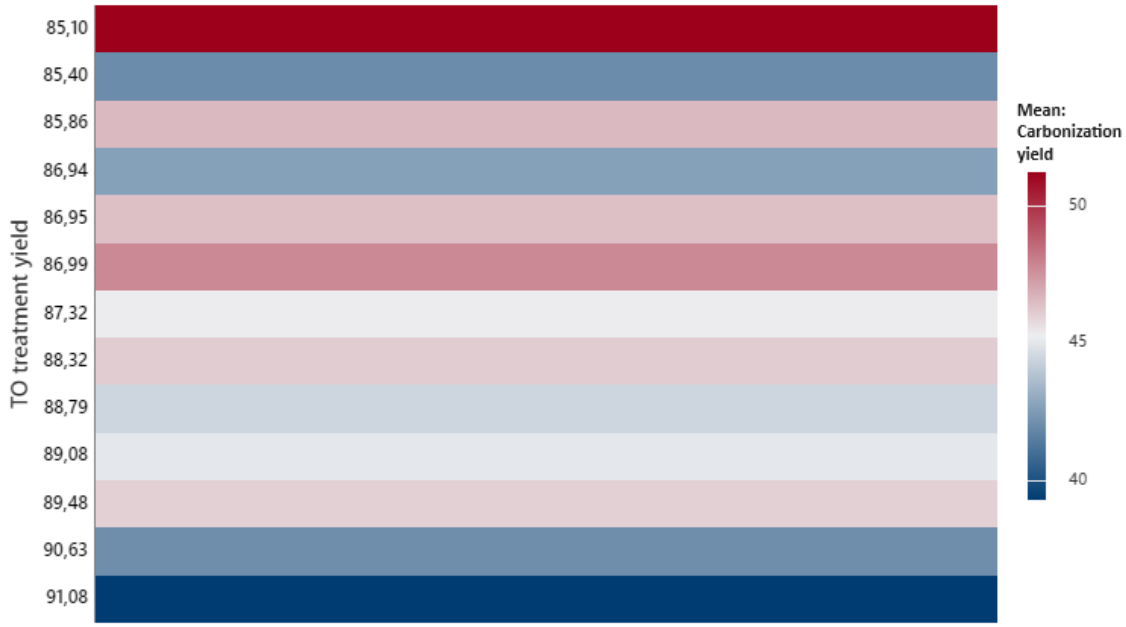

Figure 20. Heatmap of the yield comparison

The correlation between total C% of oxidised lignin and carbonization yield also needs to be verified with more data, but it is expected that the yield is higher with higher C% after the TO treatment. Figure 21 shows a correlation between C% and the carbonization yield from current data, which supports the estimation.

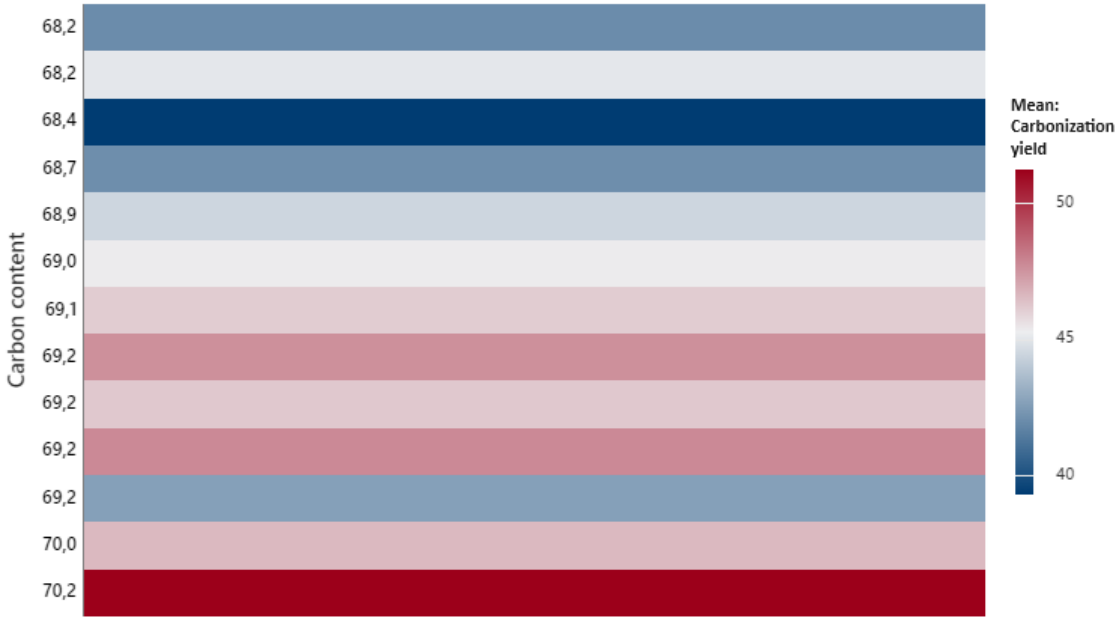

Figure 21. Heat map of carbonization yield versus C%

Accurate regression model of TO treatment yield and/or total C% measured with OEA could help estimate carbonization yield after following process steps. Maximizing carbonization yield for carbon-based products could be crucial information, when investigating investment profitability for future production plants.

It is known that that TO treatment improves the processability by preventing melting in later processing steps, but the needed degree of the TO treatment and crosslinking remains indeterminate. Yuan et al. (2017) studied TO treatment for pitch-based CF precursors discovered that TO treatment conditions have a significant influence on the thermal decomposition behaviour in carbonization process, and on the final electrical and mechanical properties of the carbon. These properties are also essential in lignin derived, carbon-based applications like CF and battery materials. Consequently, achieving fully crosslinked lignin was the primary goal.

In this study, MDSC measurements of the T_g and reaction energy (non-reversing energy) were used to estimate the degree of TO treatment and crosslinking. Missing T_g and reaction energy from some samples complicated the data analysis somewhat, but the model was formed and can be made more fitting with more data.

The main effects for significant responses of the three chosen factors were identified, especially the T_g value was of interest. Key parameter settings were also identified with response optimization; thus, all research questions were answered. The idea of including reaction energy for crosslinking determination was introduced in the later part of the study, so there's a great potential for future studies focusing on that.

The real effect of T_g and reaction energy can be seen in the later process steps and in the performance of the finished product. The research on TO treatment, however, progresses slowly since lignin goes through multiple process phases before and after the finished product. From the results of this study, future steps and next set of trials with new parameter values can already be concluded. For example, it would be beneficial to study the effect of HR more. If heating curve would steadily decrease as temperature rises, processing time could decrease without negative impact on quality of crosslinking.

Although our results mostly correspond with the other studies, every study used different kinds of lignin. Lignin properties are complex and vary based on source, separation method and conversion processes. Also, different form of lignin and processing methods were used, e.g., Cho et al. (2019) used lignin nanofibers and fiber mats for the TO treatment and Brodin et al. (2012) studied TO treatment for three different lignin sources in powder form.

The design of TO treatment for specific properties of lignin would also benefit from understanding the chemical reactions occurring in the TO treatment. It would have been beneficial in our study to perform FT-IR and/or NMR spectroscopy for the samples and raw material to compare, what kind of modification the TO treatment has made to the structure of lignin. Most studies regarding the TO treatment, including Braun et al. (2005) and Brodin et al. (2012), used various spectroscopy methods to identify functional groups. It is expected that results would be similar to the other studies, but as mentioned, differences in raw material type could bring forth new discoveries.

For future research, it would be interesting to investigate the TO treatment behaviour in more oxygen-rich environment. Before mentioned Poletto (2018) stated that the use of strong oxidants breaks up the aromatic ring of the polymer, whereas milder ones, like air, changes only its functional groups. TO-related reactions could be accelerated and controlled if pure oxygen would be mixed with air. The amount of oxygen could be optimized up to point

where aromatic rings won't break, but TO-related reactions are accelerated and processing time shortened.

Behaviour of other types of lignin are also of interest. Xu & Ferdosian (2017) mention enzymatic hydrolysis lignin (EHL) as a type of lignin isolated as an insoluble residue and describes separation method as it "normally operates under relatively mild conditions, the most active functional groups such as phenolic hydroxyl and alcoholic hydroxyl can be preserved. As a consequence, the resulting EHL is expected to be more reactive in comparison with lignosulfonate or kraft lignin." Hydroxyl groups are oxidized to carbonyl groups in the TO treatment, and a larger amount of hydroxyl groups could positively impact the TO-treated lignin.

It is crucial to understand the raw material well in order to optimize i.e., find a balance between good quality and cost-effective processing, to produce value-added products. The mechanisms of the TO reactions are still not completely understood due to its complexity, and so TO conditions can been mainly selected from examination of the structure and properties of the resulting treated lignin.

The demand for new, green chemicals and products has risen in recent years due to climate change and rising costs but also with the need to cut carbon emissions due to EU regulation. CO_2 emissions in the pulp and paper industry arise mostly in the production of energy. In the near future burning lignin for energy may not be as profitable as creating new products from lignin.

Some modern biorefineries also have the possibility to produce low to high-value compounds from lignin at low-cost and stable basis but are still not feasible. Demand for lignin in value-added products could represent an opportunity to boost the competitiveness and economic feasibility of the future lignocellulosic biorefineries (Bajwa et al., 2019).

References

Bajpai, P. (Pratima) (2017) Carbon Fibre from Lignin. Springer Singapore. https://doi.org/10.1007/978-981-10-4229-4

Bajwa, D. S. et al. (2019) A concise review of current lignin production, applications, products and their environmental impact. Industrial Crops and Products, 139, 111526-. https://doi.org/10.1016/j.indcrop.2019.111526

Bhattacharyya, S. et al. (2020) Melt Stable Functionalized Organosolv and Kraft Lignin Thermoplastic. Processes. [Online] 8 (9), 1108-. https://doi.org/10.3390/pr8091108

Beste, A. (2014) ReaxFF Study of the Oxidation of Softwood Lignin in View of Carbon Fiber Production. *Energy & Fuels*, *28*(11), 7007–7013. https://doi.org/10.1021/ef501901p

Braun, J. L. et al. (2005) Lignin-based carbon fibers: Oxidative thermostabilization of kraft lignin. Carbon (New York), 43(2), 385–394. https://doi.org/10.1016/j.carbon.2004.09.027

Brodin, I. et al. (2012) Oxidative stabilisation of kraft lignin for carbon fibre production. Holzforschung. 66. 141-147. DOI: 10.1515/HF.2011.133.

Chatterjee, S. & Saito, T. (2015) Lignin-Derived Advanced Carbon Materials. ChemSusChem; ChemSusChem, 8(23), pp. 3941-3958. https://doi-org.ezproxy.cc.lut.fi/10.1002/cssc.201500692

Cho, M. et al. (2019) Impact of Thermal Oxidative Stabilization on the Performance of Lignin-Based Carbon Nanofiber Mats. ACS omega. [Online] 4 (3), 5345–5355. https://doi.org/10.1021/acsomega.9b00278

Du, Y.-F. et al. (2021) Pre-oxidation of lignin precursors for hard carbon anode with boosted lithium-ion storage capacity. Carbon (New York), 178, 243–255. https://doi.org/10.1016/j.carbon.2021.03.016

Ekielski, A., Mishra, P.K. (2021) Lignin for Bioeconomy: The Present and Future Role of Technical Lignin. Int. J. Mol. Sci. 2021, 22, 63. https://doi.org/10.3390/ijms22010063

Engineers Academy. (2018) Properties of Amorphous and Crystalline Polymers. Available in (https://www.youtube.com/watch?v=9yVywEMutSY) (Accessed 21.5.2024)

Hasan, G. et al. (2020) Role of different lignin systems in polymers: mechanical properties and thermal stability. Polish Journal of Chemical Technology, 22(4), 10–16. https://doi.org/10.2478/pjct-2020-0032

Jiju A. (2023) Design of Experiments in the service industry: a critical literature review and future research directions. Design of Experiments for Engineers and Scientists (Third Ed.). Chapter 12. ISBN: 9780443151736

Lin, X. et al. (2020) Advanced lignin-derived hard carbon for Na-ion batteries and a comparison with Li and K ion storage. Carbon (New York). [Online] 157316–323. https://doi-org.ezproxy.cc.lut.fi/10.1002/cssc.201500692

Poletto, M. (2018) Lignin: trends and applications (M. Poletto, Ed.; 1st ed.). IntechOpen. DOI: 10.5772/intechopen.70376

Statistical Modeling. (n.d.) Minitab help. Minitab support site. Cited 4.6.2024. Available in Support.minitab.com

Suota, M. J. et al. (2021) Chemical and structural characterization of hardwood and softwood LignoForceTM lignins. Industrial Crops and Products, 173,114138-. https://doi.org/10.1016/j.indcrop.2021.114138

TA Instruments. (2005) Modulated DSC® Paper #1. Why Modulated DSC®? An Overview and Summary of Advantages and Disadvantages Relative to Traditional DSC. Cited 2.6.2024. Available in TP_006_MDSC_num_1_MDSC.pdf (tainstruments.com)

TA Instruments. (2006). Getting started quide Q500. Q Series™. Waters LLC. Operations manual. Cited 20.5.2024. Available in TGA Q Series Getting Started Guide (usf.edu)

TA Instruments. (2007). Getting started quide Q2000. Q Series™. Waters LLC. Operations manual. Cited 20.5.2024. Available in DSC Q Series Getting Started Quide (nmt.edu)

Thermo Fisher Scientific – Handheld Elemental & Radiation Detection. (2020, December 01) OES, XRF, and LIBS: What's the Difference?. AZoM. Cited 29.5.2024. available in https://www.azom.com/article.aspx?ArticleID=19893

Thomas, J. et al. (2021) Crosslinkable Polyethylene: Manufacture, Properties, Recycling, and Applications. 1st Edition 2021. [Online]. Singapore: Springer Singapore Pte. Limited. https://doi.org/10.1007/978-981-16-0514-7

Xu, C., Ferdosian, F. (2017) Conversion of Lignin into Bio-Based Chemicals and Materials. Springer Berlin Heidelberg. https://doi.org/10.1007/978-3-662-54959-9

Yuan, G. et al. (2017) A comprehensive study on the oxidative stabilization of mesophase pitch-based tape-shaped thick fibers with oxygen. Carbon (New York). [Online] 11559–76. https://doi.org/10.1016/j.carbon.2016.12.040

Zhao, F. et al. (2018) Recent Advances in Applying Vulcanization/Inverse Vulcanization Methods to Achieve High-Performance Sulfur-Containing Polymer Cathode Materials for Li–S Batteries. Small methods. [Online] 2 (11). https://doi.org/10.1002/smtd.201800156

Appendix 1. Comparison of MDSC data

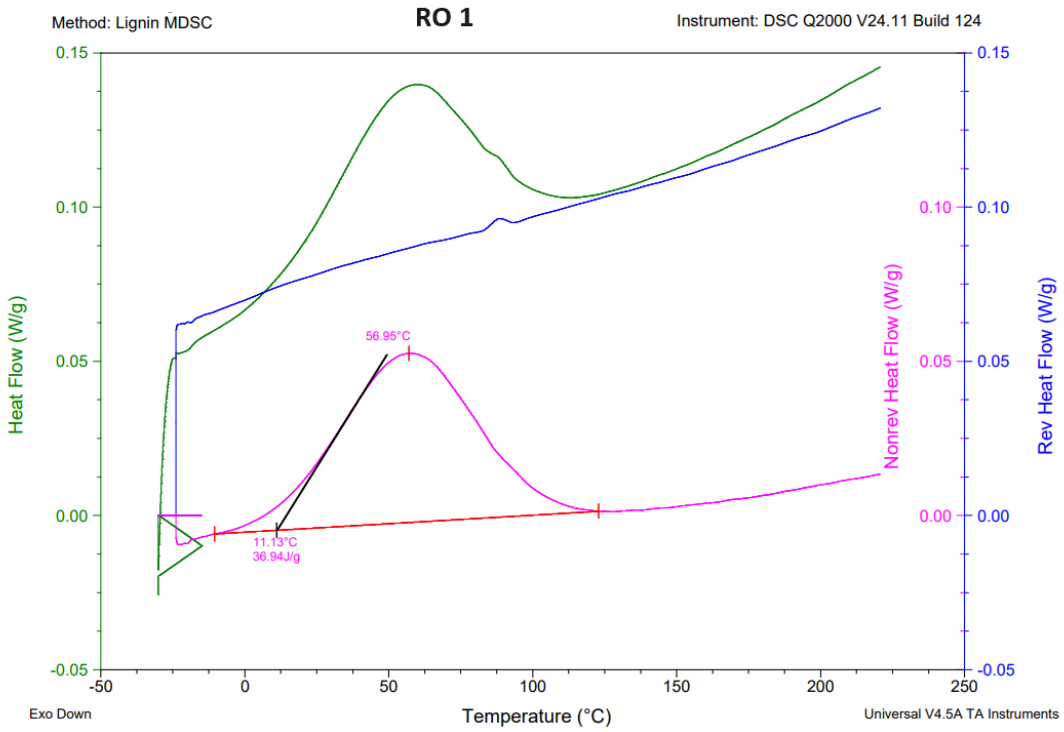

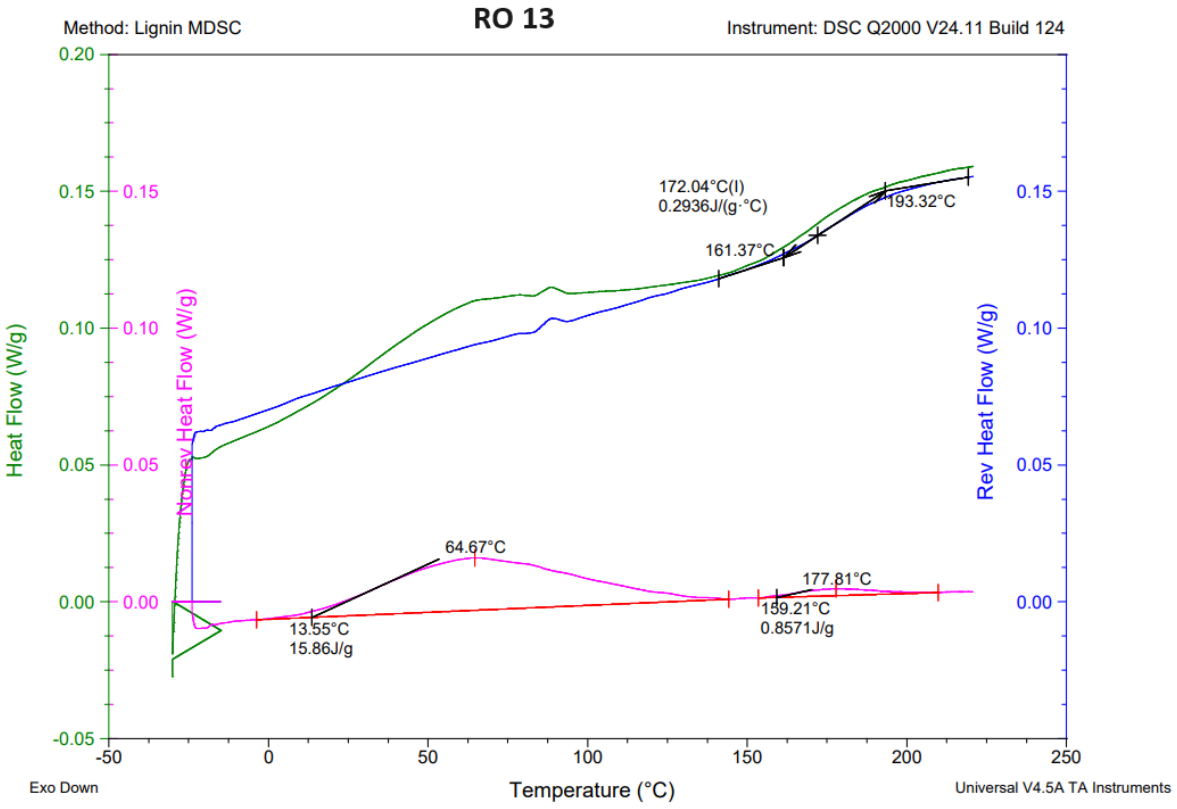

Appendix 2. Factorial regression of glass-transition temperature T_g

Model Summary

S	R-sq	R-sq(adj)	R-sq(pred)
2,15788	93,02%	90,23%	69,45%

Analysis of Variance

Source	DF	Adj SS	Adj MS	F-Value	P-Value
Model	2	310,446	155,223	33,34	0,001
Linear	2	310,446	155,223	33,34	0,001
Temperature	1	131,869	131,869	28,32	0,003
Holding time	1	265,660	265,660	57,05	0,001
Error	5	23,282	4,656		
Curvature	1	11,146	11,146	3,67	0,128
Lack-of-Fit	2	3,107	1,554	0,34	0,744
Pure Error	2	9,029	4,515		
Total	7	333,728			

Regression Equation in Uncoded Units

Tg mean = 97,0 + 0,3073 Temperature + 3,275 Holding time

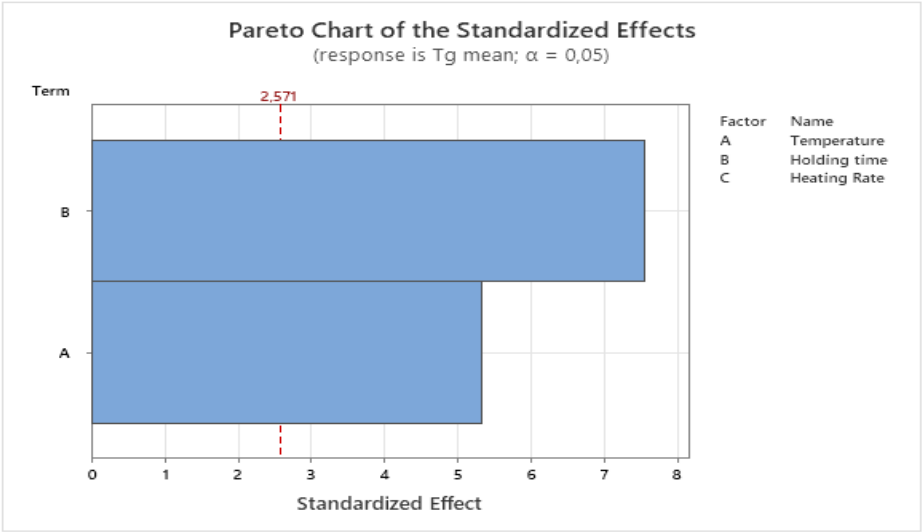

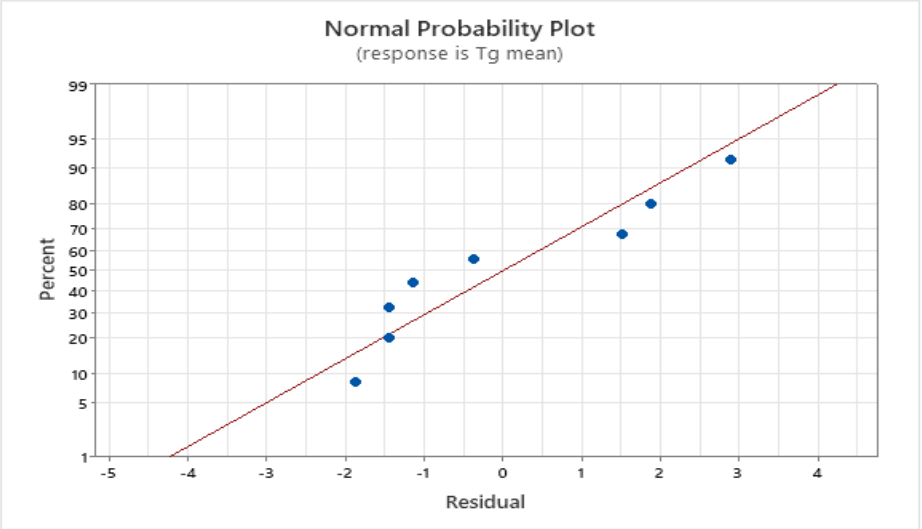

Appendix 3. Factorial regression of carbonization yield

Model Summary

S	R-sq	R-sq(adj)	R-sq(pred)
0,591243	97,59%	96,09%	92,74%

Analysis of Variance

Source	DF	Adj SS	Adj MS	F-Value	P-Value
Model	5	113,308	22,6615	64,83	0,000
Linear	3	108,172	36,0573	103,15	0,000
Temperature	1	45,982	45,9817	131,54	0,000
Holding time	1	54,105	54,1051	154,78	0,000
Heating Rate	1	26,345	26,3446	75,36	0,000
2-Way Interactions	1	4,441	4,4408	12,70	0,007
Temperature*Heating Rate	1	4,441	4,4408	12,70	0,007
Curvature	1	0,695	0,6949	1,99	0,196
Error	8	2,797	0,3496		
Lack-of-Fit	3	0,864	0,2878	0,74	0,570
Pure Error	5	1,933	0,3866		
Total	13	116,104			

Regression Equation in Uncoded Units

TGA yield = 3,59 + 0,1587 Temperature + 1,1261 Holding time + 6,34 Heating Rate
- 0,03042 Temperature*Heating Rate + 0,637 Ct Pt

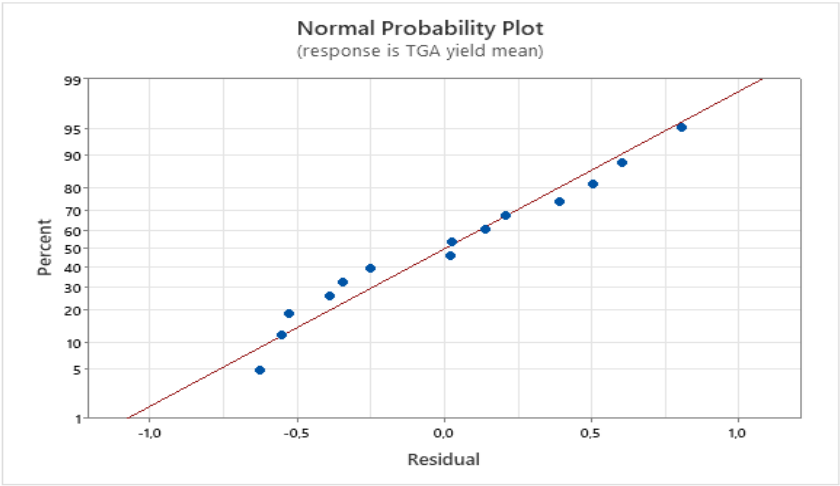

Appendix 4. Factorial regression of carbon content

Model Summary

S	R-sq	R-sq(adj)	R-sq(pred)
0,313156	76,64%	69,63%	51,49%

Analysis of Variance

Source	DF	Adj SS	Adj MS	F-Value	P-Value
Model	3	3,21731	1,07244	10,94	0,002
Linear	3	3,21731	1,07244	10,94	0,002
Temperature	1	2,35558	2,35558	24,02	0,001
Holding time	1	0,81894	0,81894	8,35	0,016
Heating Rate	1	0,24671	0,24671	2,52	0,144
Error	10	0,98067	0,09807		
Curvature	1	0,00135	0,00135	0,01	0,914
Lack-of-Fit	4	0,28997	0,07249	0,53	0,723
Pure Error	5	0,68934	0,13787		
Total	13	4,19798			

Regression Equation in Uncoded Units

Carbon content = 63,17 + 0,02215 Temperature + 0,1385 Holding time - 0,1521 Heating Rate

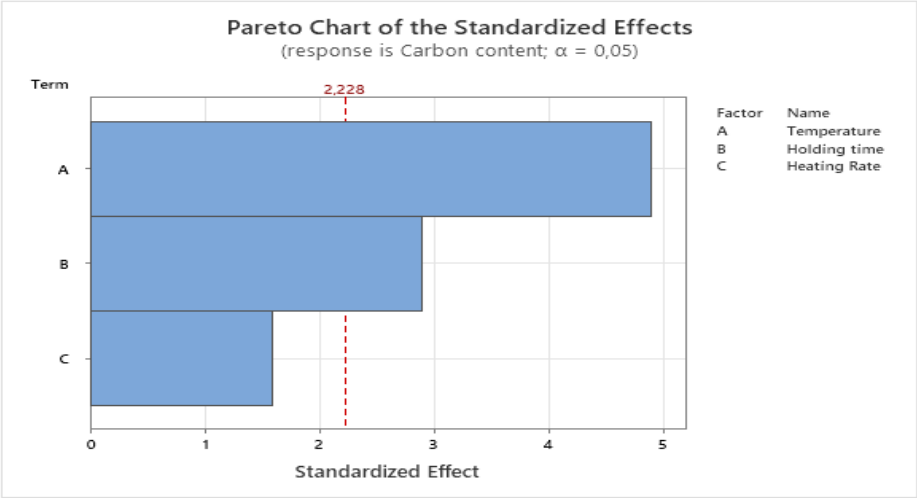

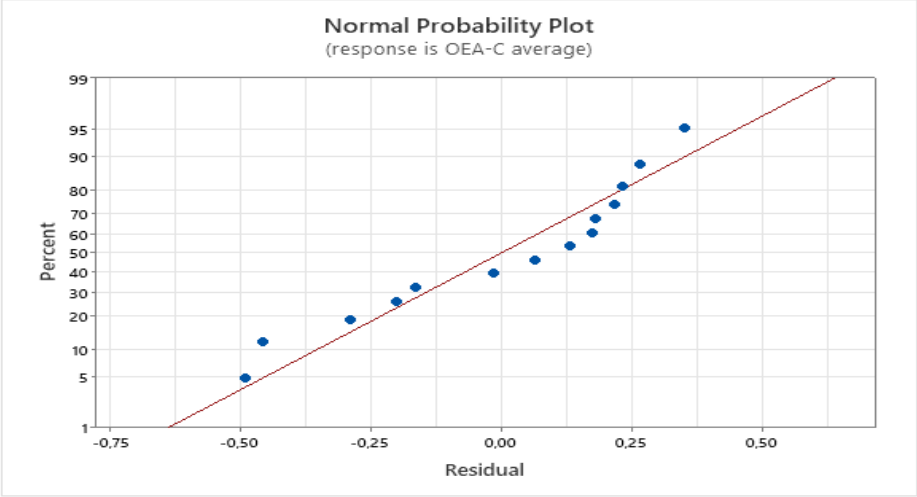

Appendix 5. Factorial regression of oxygen content

Model Summary

S	R-sq	R-sq(adj)	R-sq(pred)
0,238175	65,78%	59,56%	41,25%

Analysis of Variance

Source	DF	Adj SS	Adj MS	F-Value	P-Value
Model	2	1,19963	0,59982	10,57	0,003
Linear	2	1,19963	0,59982	10,57	0,003
Temperature	1	1,11630	1,11630	19,68	0,001
Holding time	1	0,08333	0,08333	1,47	0,251
Error	11	0,62400	0,05673		
Curvature	1	0,00039	0,00039	0,01	0,939
Lack-of-Fit	5	0,14712	0,02942	0,31	0,889
Pure Error	5	0,47650	0,09530		
Total	13	1,82364			

Regression Equation in Uncoded Units

oxygen content = 26,878 - 0,01525 Temperature - 0,0417 Holding time

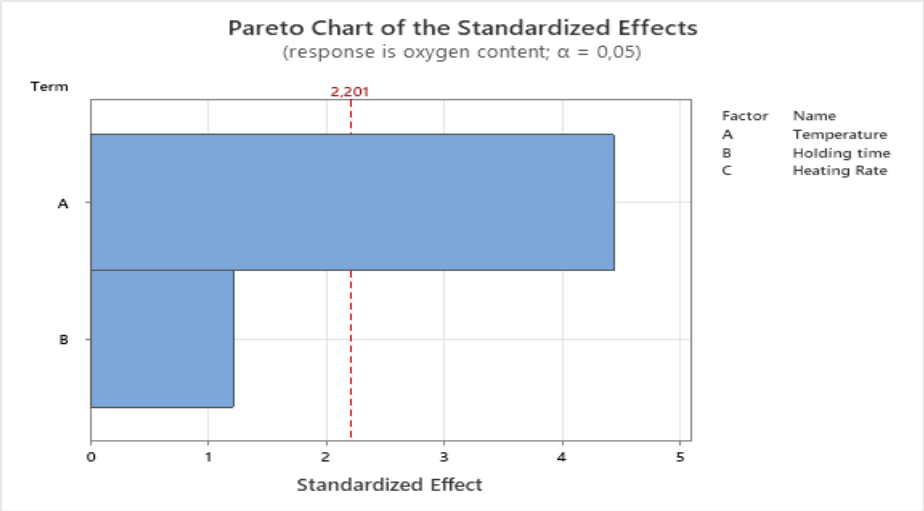

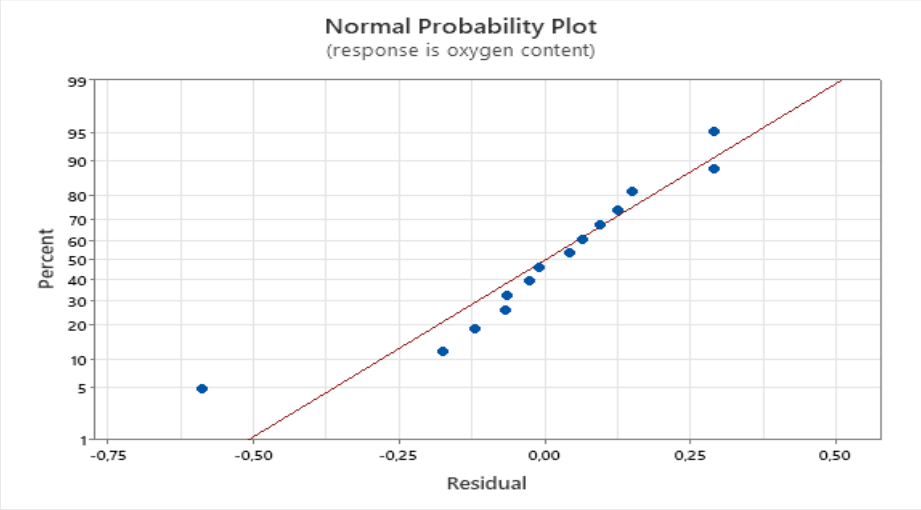

Appendix 6. Factorial regression of reaction energy

Model Summary

S	R-sq	R-sq(adj)	R-sq(pred)
0,103032	94,72%	90,50%	21,24%

Analysis of Variance

Source	DF	Adj SS	Adj MS	F-Value	P-Value
Model	4	0,95213	0,238032	22,42	0,002
Linear	3	0,82747	0,275823	25,98	0,002
Temperature	1	0,01819	0,018186	1,71	0,248
Holding time	1	0,03887	0,038868	3,66	0,114
Heating Rate	1	0,76889	0,768888	72,43	0,000
2-Way Interactions	1	0,32499	0,324990	30,61	0,003
Temperature*Heating Rate	1	0,32499	0,324990	30,61	0,003
Error	5	0,05308	0,010616		
Curvature	1	0,03611	0,036109	8,51	0,043
Lack-of-Fit	1	0,00075	0,000750	0,14	0,734
Pure Error	3	0,01622	0,005407		
Total	9	1,00521			

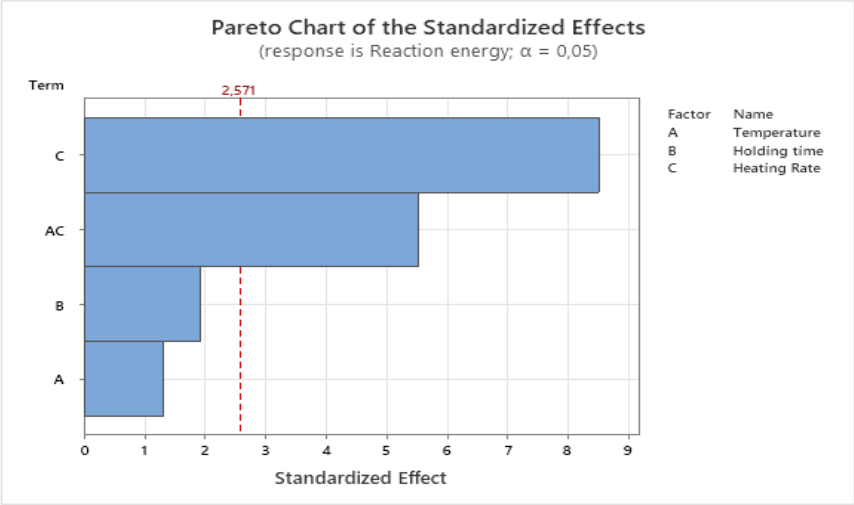

Regression Equation in Uncoded Units

Reaction energy = 6,738 - 0,02405 Temperature - 0,0418 Holding time - 2,432 Heating Rate
+ 0,01062 Temperature*Heating Rate

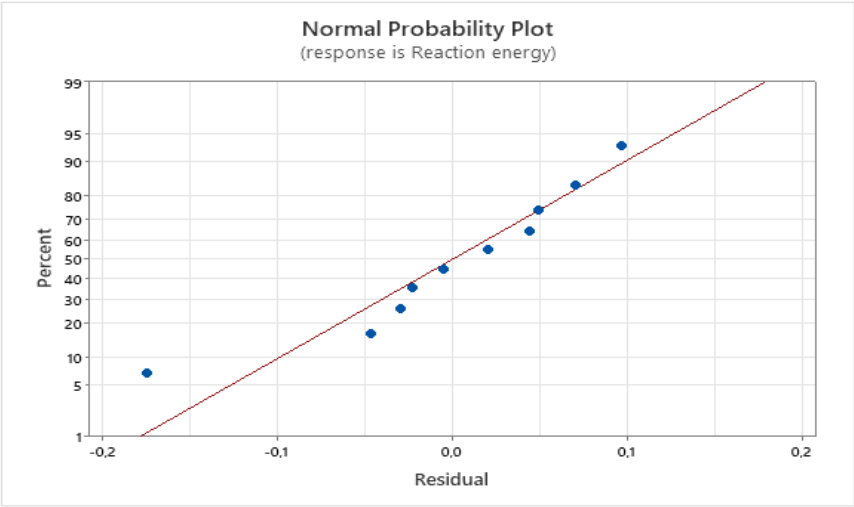

Appendix 7. Factorial regression of TO treatment yield

Model Summary

S	R-sq	R-sq(adj)	R-sq(pred)
0,359780	97,03%	96,44%	95,47%

Analysis of Variance

Source	DF	Adj SS	Adj MS	F-Value	P-Value
Model	2	42,3240	21,1620	163,49	0,000
Linear	2	42,3240	21,1620	163,49	0,000
Temperature	1	38,1878	38,1878	295,02	0,000
Holding time	1	6,9332	6,9332	53,56	0,000
Error	10	1,2944	0,1294		
Curvature	1	0,1229	0,1229	0,94	0,357
Lack-of-Fit	5	0,5229	0,1046	0,64	0,683
Pure Error	4	0,6486	0,1622		
Total	12	43,6184			

Regression Equation in Uncoded Units
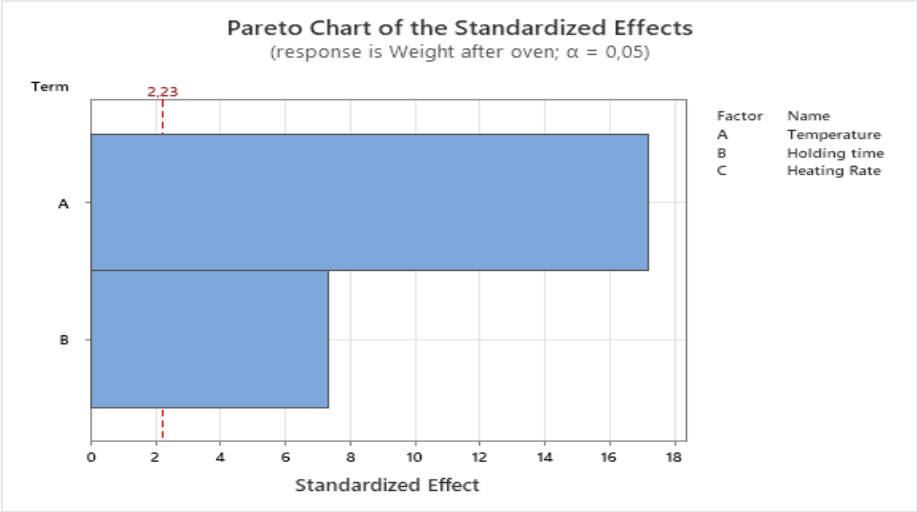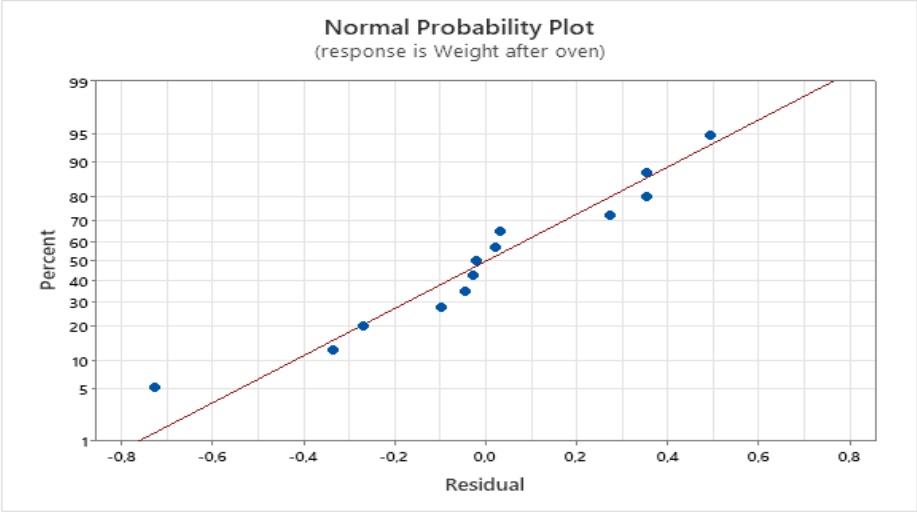
Weight after oven = 113,67 - 0,09395 Temperature - 0,4003 Holding time